Astroparticle and particle physics at ultra high energies: selected results and perspectives from the Pierre Auger Observatory

Antonella Castellina

INFN & INAF, Torino, Italy

Vulcano Workshop, 23-28 May 2016

The scientific case for Auger

assess the existence or absence of the cut-off

measure the anisotropy in the quest for the sources

find out the nature of the primary cosmic rays

... with a hybrid detector

...the scientific case for the upgrade

origin of the cut-off : GZK or Emax ?

the proton fraction at UHE: particle astronomy?

hadronic interaction models : new physics ?

... improving the composition knowledge at UHE

Models for origin, acceleration, propagation of Galactic and extragalactic CRs

- Ankle at 4.8×10^{18} eV
- Cut-off (>20σ C.L.), $E_{1/2} = 2.4 \times 10^{19}$ eV
- Composition lighter from 10^{17} to $10^{18.3}$ eV, heavier above. Mixed at ankle.
- ~10% protons at >2-3 10^{19} eV
- anisotropy: large, intermediate, small scale results

and more....

- Elves, sprites
- solar physics

particle physics

- smooth growth of the pp cross section (meas. 57 TeV)
- constraints to the hadronic interaction models from muon measurements
- constraints to hadronic interaction models from em and muonic longitudinal development
- new models tuned on air showers used at LHC
- fundamental physics

ν, γ

- Limits on primary photons: exclusion of top-down models
- No photons/neutrons from Galactic sources
- Neutrinos constraints on astrophysical models
- correlation studies with TA and Icecube
- constraints on em counterparts of GW

The Pierre Auger Observatory

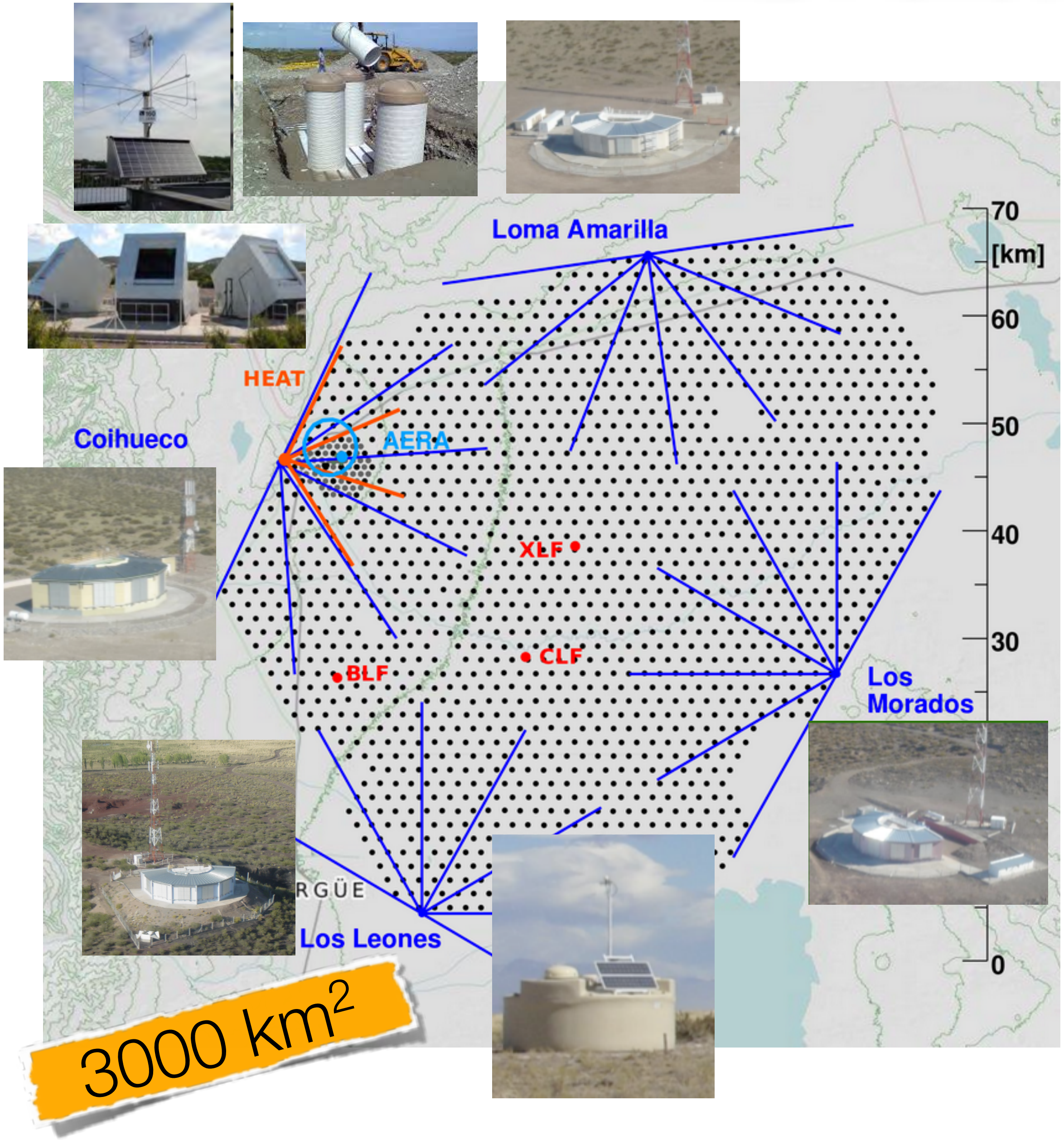

- Water-Cherenkov tanks
  - 1660 in a 1.5 km standard grid
  - 71 in 0.75 km infill grid (~30 km^2)
- Fluorescence Telescopes
  - 24 in 4 buildings overlooking SD
  - 3 in 1 building overlooking the Infill
- Underground Muon detectors
  - engineering array phase - 61 aside the Infill stations
- AERA radio antennas
  - 153 graded 17 km^2
- atmospheric monitoring stations

Shower Observables in a hybrid detector

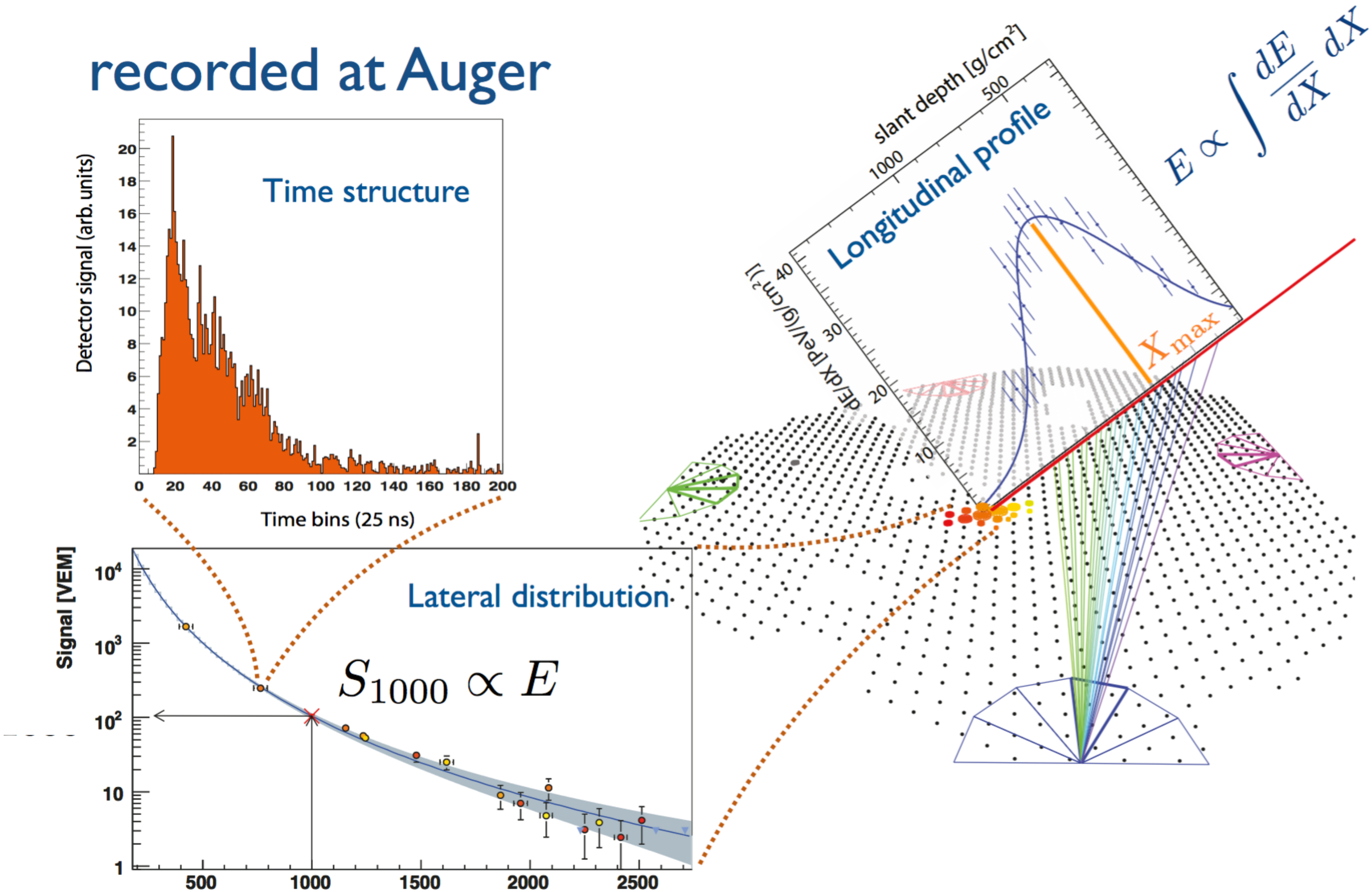

SD	
SD annual exposure, $\theta < 60°$	$\sim$5500 km^2 sr yr
T3 rate	0.1 Hz
T5 events/yr, $E > 3$ EeV	$\sim$14,500
T5 events/yr, $E > 10$ EeV	$\sim$1500
Reconstruction accuracy (S_{1000})	22% (low E) to 12% (high E)
Angular resolution	1.6° (3 stations) 0.9° (> 5 stations)
Energy resolution	16% (low E) to 12% (high E)
FD	
On-time	$\sim$15%
Rate per building	0.012 Hz
Rate per HEAT	0.026 Hz
Hybrid	
Core resolution	50 m
Angular resolution	0.6°
Energy resolution (FD)	8%
X_{max} resolution	$<$20 g/cm^2

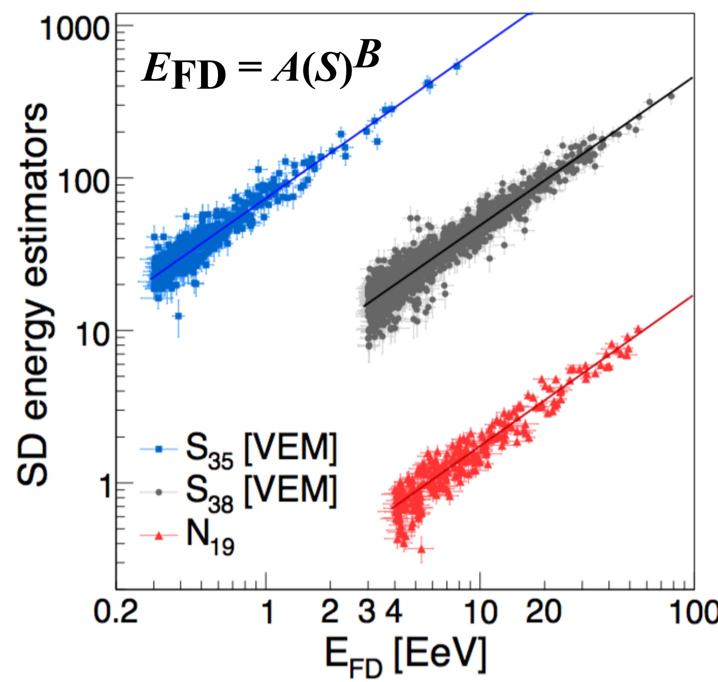

Systematic uncertainty on energy scale	**14%**
Fluorescence yield	3.6%
Atmosphere	3.4-6.2%
FD calibration	9.9%
FD profile reconstruction	6.5-5.6%
Invisible energy	3.0-1.5%
Stability of energy scale	5%
…..	

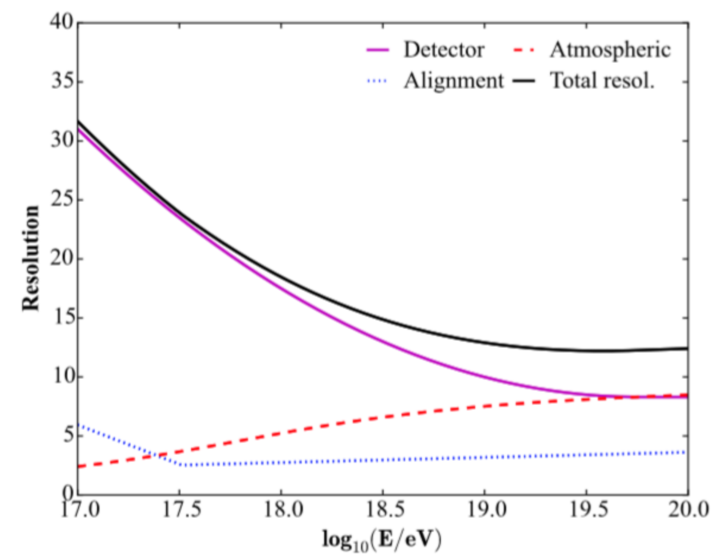

Pierre Auger Coll., Nucl.Instr.Meth.798 (2015) 172.

[I. Valino, ICRC2015, arXiv:1509.03732v1]

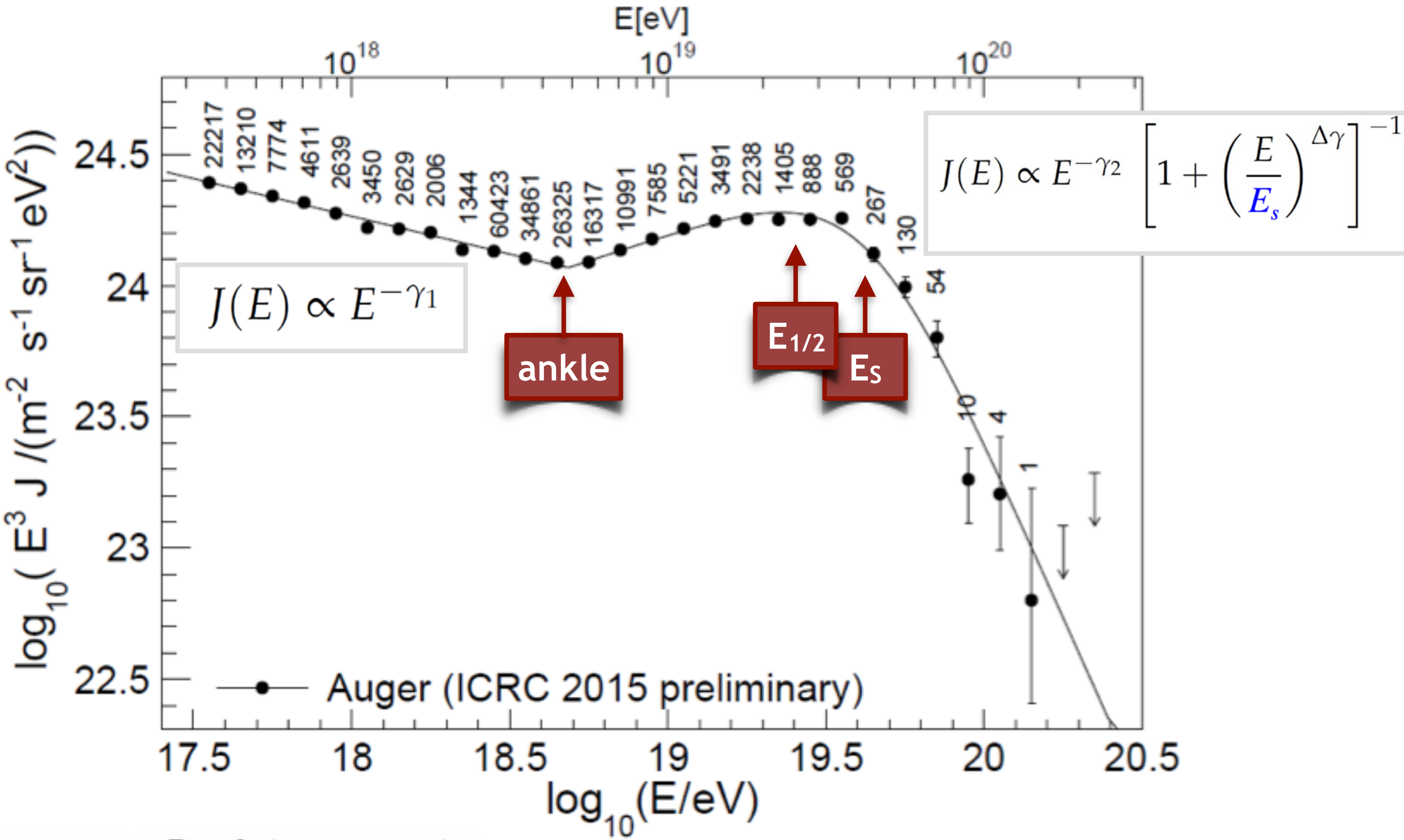

Parameter	Result ($\pm\sigma_{stat} \pm \sigma_{sys}$)
E_{ankle} [EeV]	$4.82 \pm 0.07 \pm 0.8$
γ_1	$3.29 \pm 0.02 \pm 0.05$
γ_2	$2.60 \pm 0.02 \pm 0.1$
E_s [EeV]	$42.09 \pm 1.7 \pm 7.61$
$\Delta\gamma$	$3.14 \pm 0.2 \pm 0.4$

$\boxed{\mathbf{E}_{1/2} = (\mathbf{24.7} \pm \mathbf{0.1}\,^{+8.2}_{-3.4})\ \mathrm{EeV}}$

- ankle and cutoff clearly observed
- fitting model: power law below the ankle+power law with smooth suppression above

Mass composition - X_{max} moments

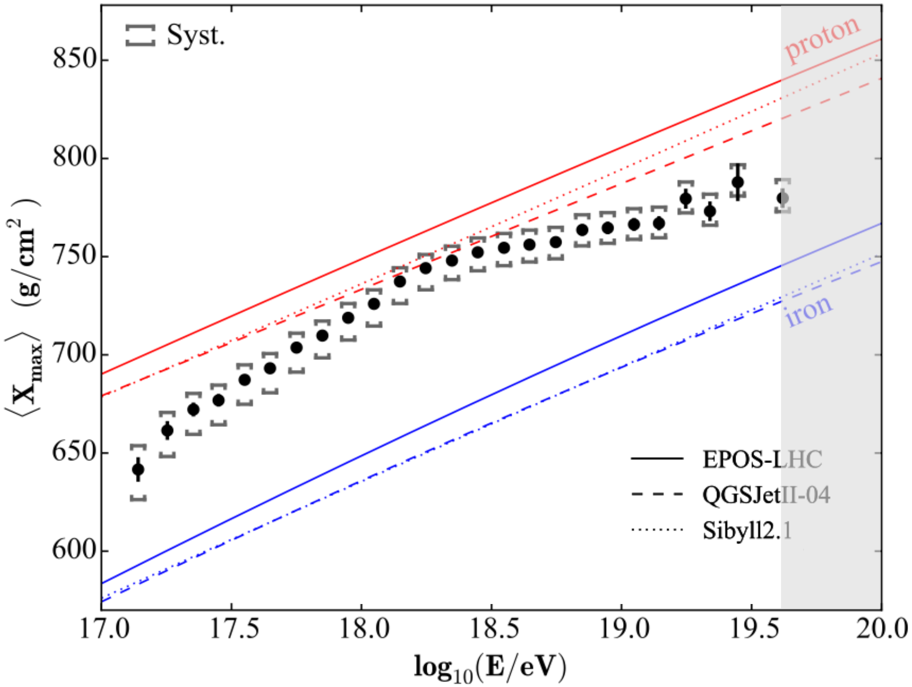

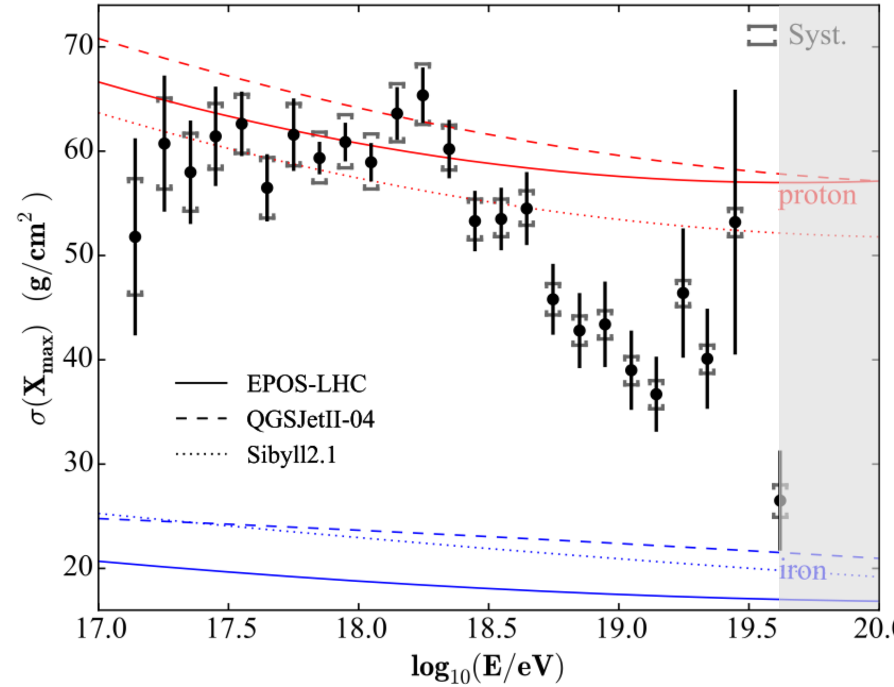

[A.Porcelli, ICRC2015, arXiv:1509.03732v1]

elongation rate not compatible with that expected from constant composition
~85 g cm^{-2} before and ~25 g cm^{-2} after the ankle

Mass composition - Auger vs TA

[M.Unger, ICRC2015, arXiv:1511.02103]

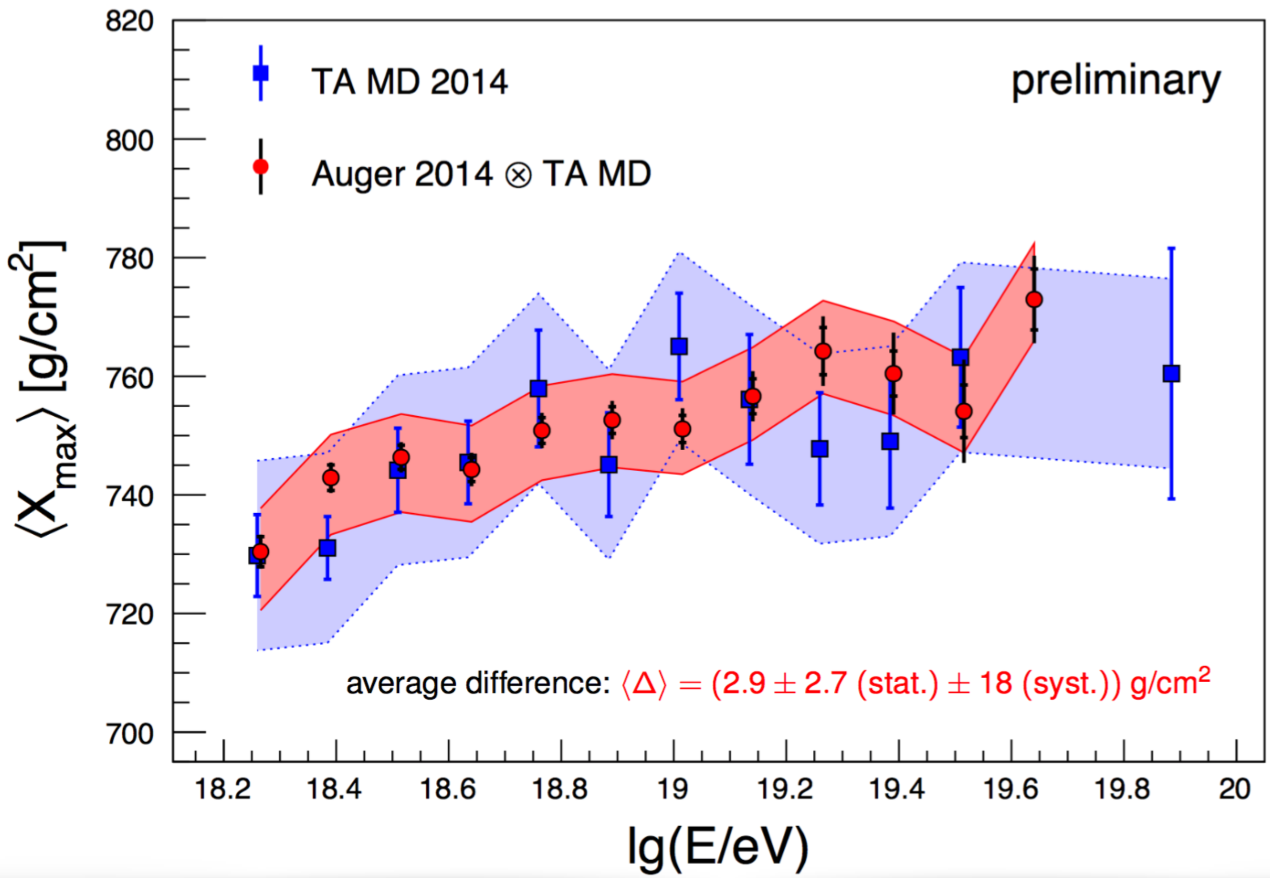

The two results are in good agreement within systematic uncertainties

TA cannot distinguish between pure proton or mixed composition with the current level of uncertainty

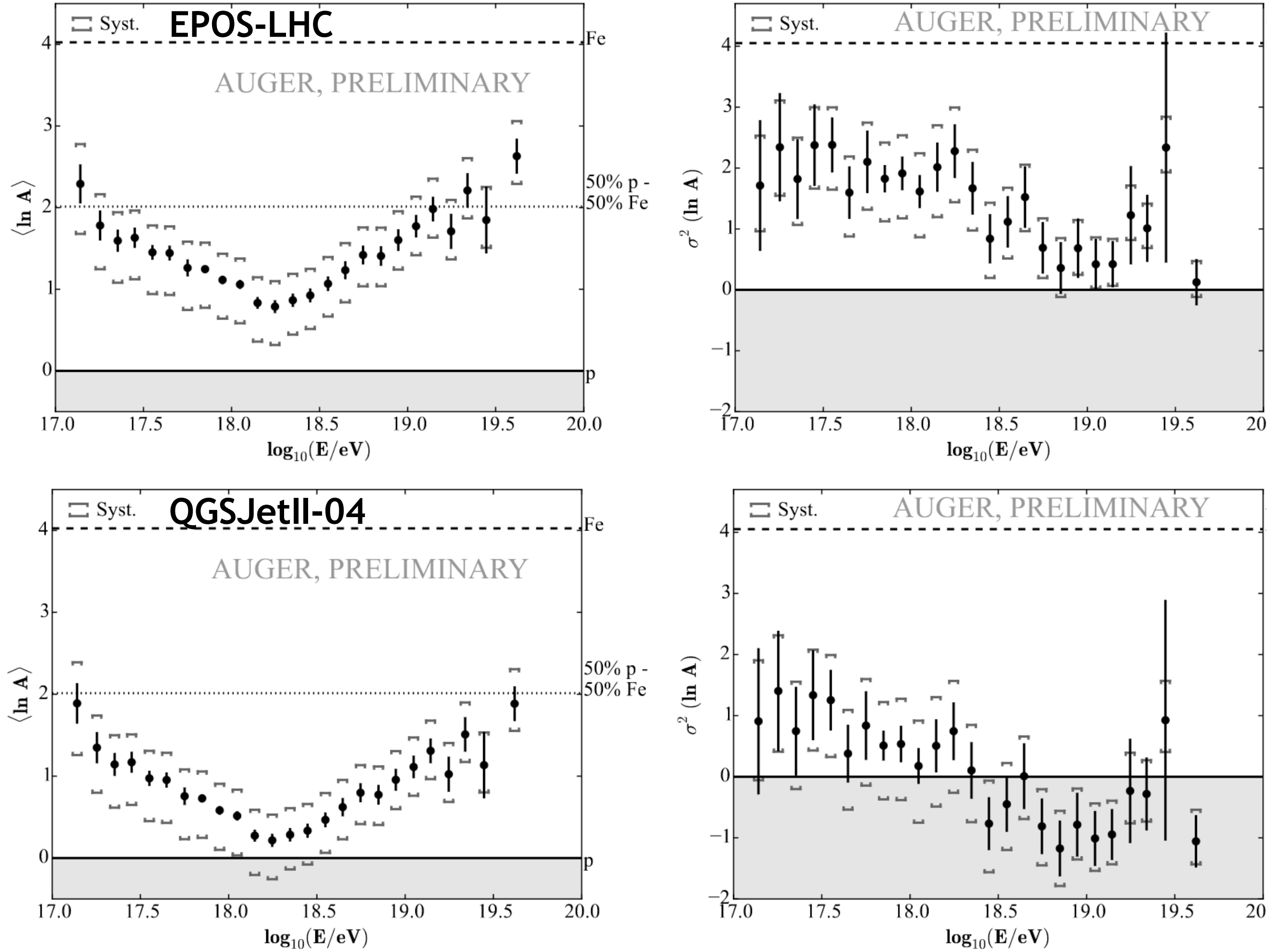

- both post-LHC models suggest heavier composition at lower energies , lightest around 2 10^{18} eV, heavier again towards highest energies
- unphysical results with QGSJetII-04 for the second moment of lnA

Mass composition - X_{max} distributions

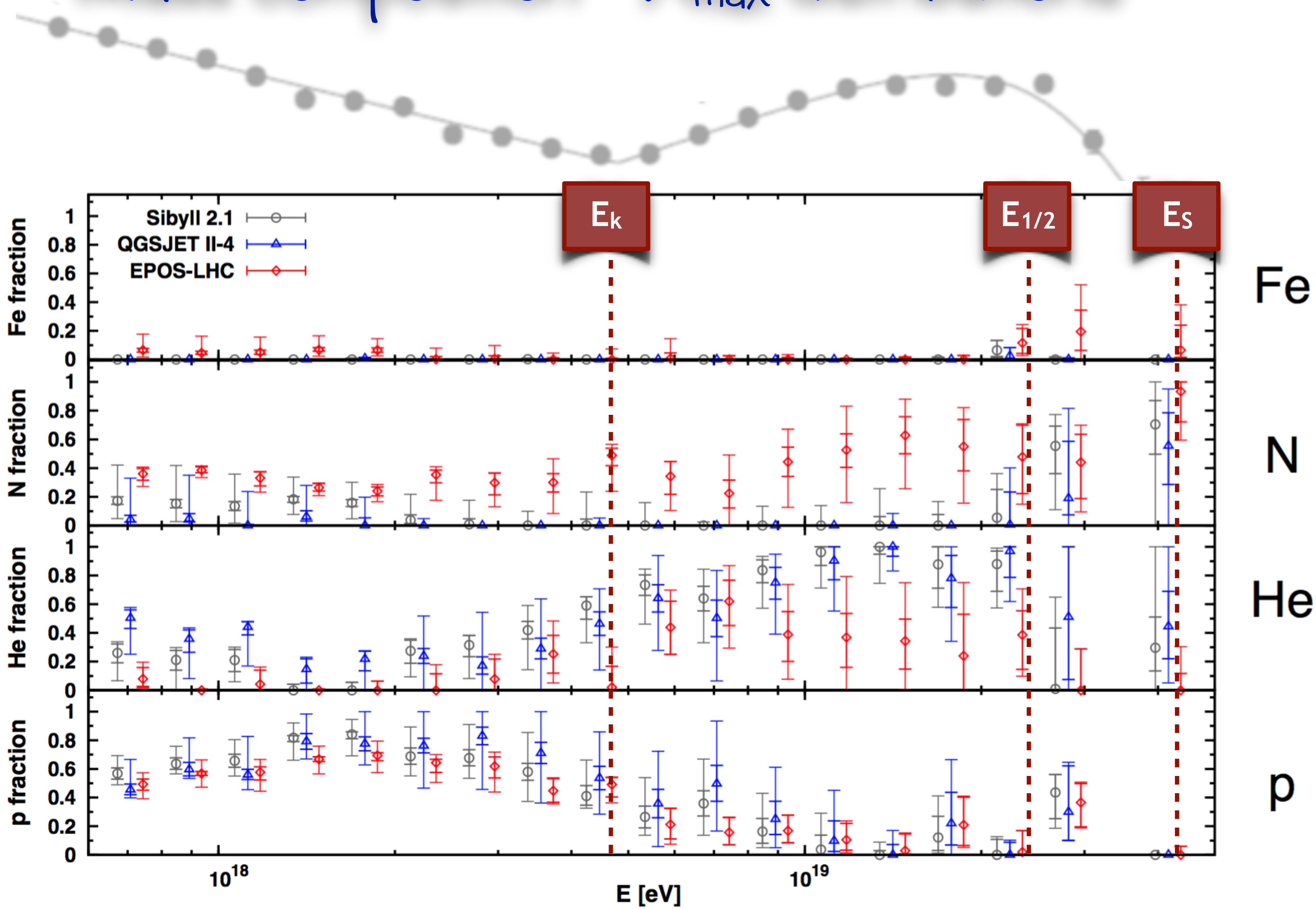

[A.Aab et al., PRD90 (2014) 122006]

Interpreting the energy spectrum

Simplified hypotheses

- identical sources homogeneously distributed
- Injection of H,He,N,Fe, injection spectrum
- Photodis.cross section + EBL (far IR)
- Propagation code: CRPropa,SimProp

$$\frac{dN_{\mathrm{inj},i}}{dE} = \begin{cases} J_0 p_i \left(\frac{E}{E_0}\right)^{-\gamma}, & E/Z_i < R_{\mathrm{cut}} \\ J_0 p_i \left(\frac{E}{E_0}\right)^{-\gamma} \exp\left(1 - \frac{E}{Z_i R_{\mathrm{cut}}}\right), & E/Z_i > R_{\mathrm{cut}} \end{cases}$$

model SPG	best fit	2nd local min
J_0 [$\mathrm{eV}^{-1}\,\mathrm{Mpc}^{-3}\,\mathrm{yr}^{-1}$]	7.17×10^{18}	4.53×10^{19}
γ	$0.94^{+0.09}_{-0.10}$	2.03
$\log_{10}(R_{\mathrm{cut}}/\mathrm{V})$	18.67 ± 0.03	19.84
p_{H}	$0.0^{+29.9}\%$	0.0%
p_{He}	$62.0^{+3.5}_{-22.2}\%$	0.0%
p_{N}	$37.2^{+4.2}_{-12.6}\%$	94.2%
p_{Fe}	$0.8^{+0.2}_{-0.3}\%$	5.8%
D/n	178.5/119	235.0/119
$D\,(J)$, $D\,(X_{\mathrm{max}})$	18.8, 159.8	14.5, 220.5
p	2.6%	5×10^{-4}

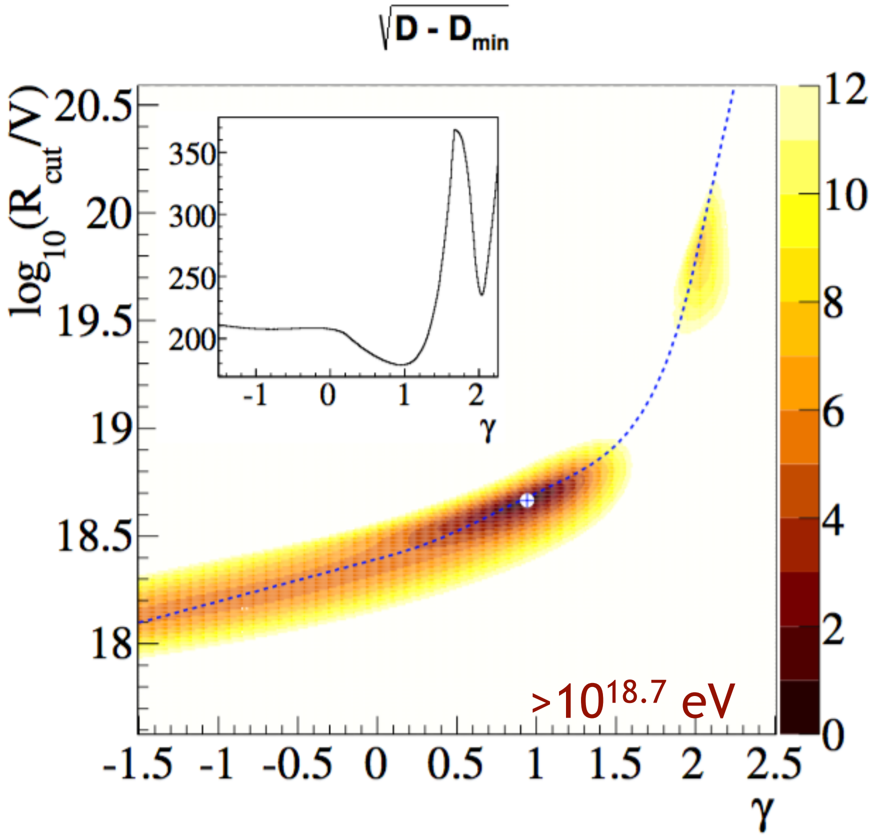

[A.di Matteo, ICRC2015, arXiv:1509.03732v1]

Interpreting the energy spectrum

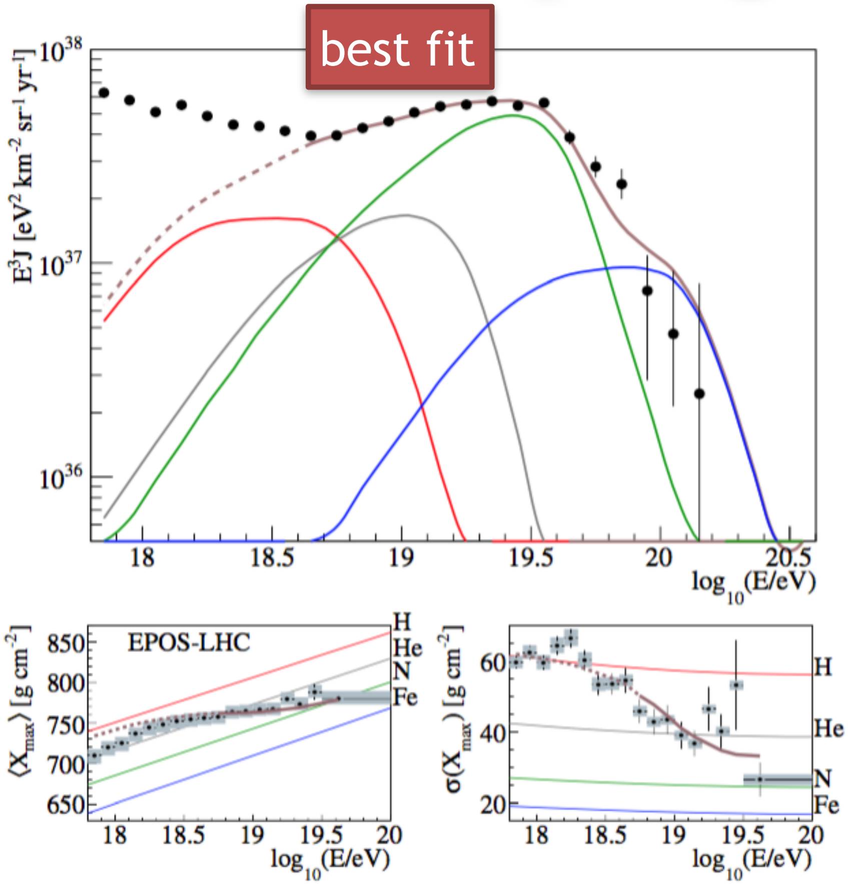

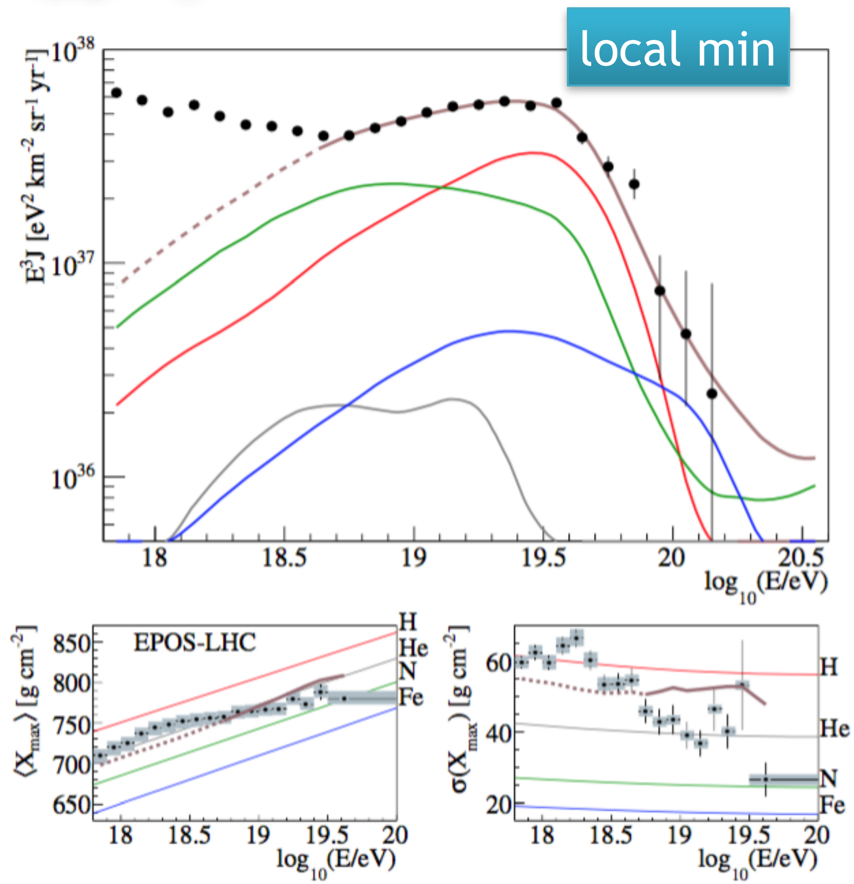

- hard injection (γ~1) and low cutoff (R_{cut}<$10^{18.7}$ eV) favoured
- γ~2 strongly disfavoured by X_{max} distribution width
- EPOS-LHC favoured over Sibyll2.1 and QGSJet04

Example scenario

(from arXiv:1505.01377)

rigidity dependent GCR component
transition from 10^{17} eV (KG light knee)
generic EGCR model

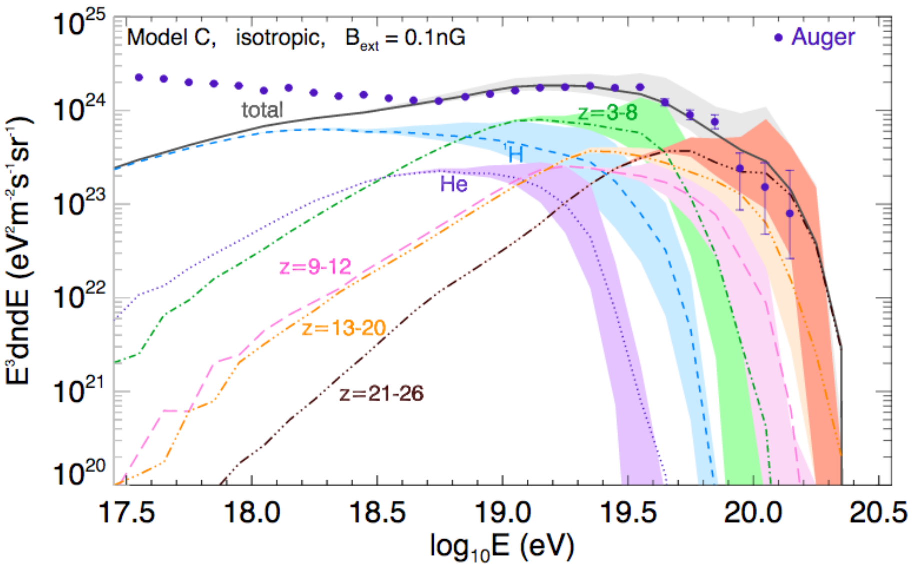

Auger $<X_{max}>$: from light to heavier above $10^{18.7}$ eV
Isotropy around the ankle

- extragalactic proton sources around the ankle, steeper spectrum (due to n)
- $Emax(Z) = Z \times Emax(A)$ + energy losses and photodissociation at sources
- strong source evolution $(1+z)^{3.5}$
- hard injection spectrum E^{-1}

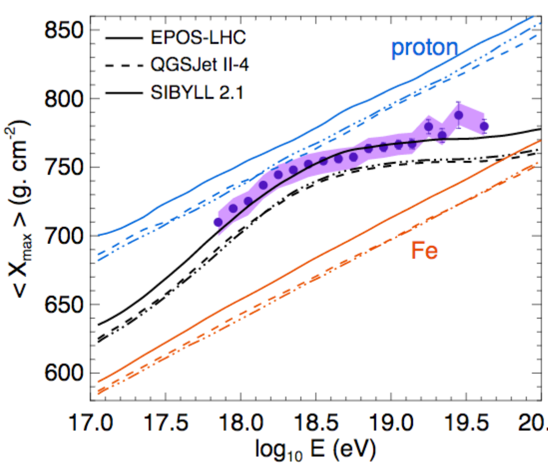

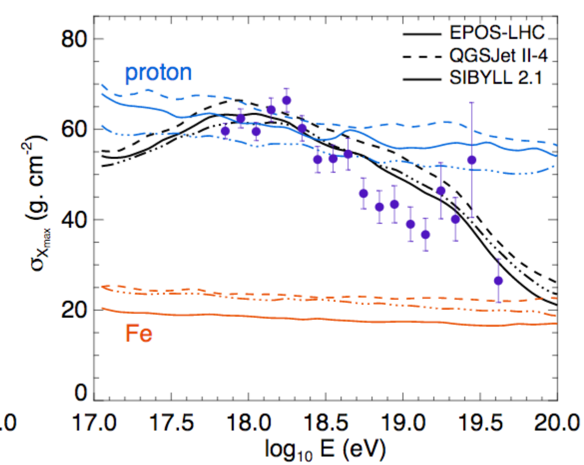

Auger X_{max} distributions:
He-N just above ankle

- dominant class of nuclei at $6\ 10^{18}$-$5\ 10^{19}$ eV medium-light

Hadronic physics with Auger

EM shower particles

X_{max}, $\sigma(X_{max})$, long.profile

- ✓ <u>high energy interactions</u> (HE γ from π^0 decay)
- ✓ profile dominated by the EM particles from secondaries in the first 100 interactions

Muons

N_μ, X^μ_{max}, $\sigma(X^\mu_{max})$, long+lat profiles

- ✓ <u>low energy interactions</u> ($\pi^\pm$ degrade to 30-100 GeV before decaying)
- ✓ negligible fraction from the first interactions

Comparison of data with expectations for

- $\sigma^2(\ln A)$
- p-Air cross section
- asymmetry of dE/dX
- muon content
- muon production depth

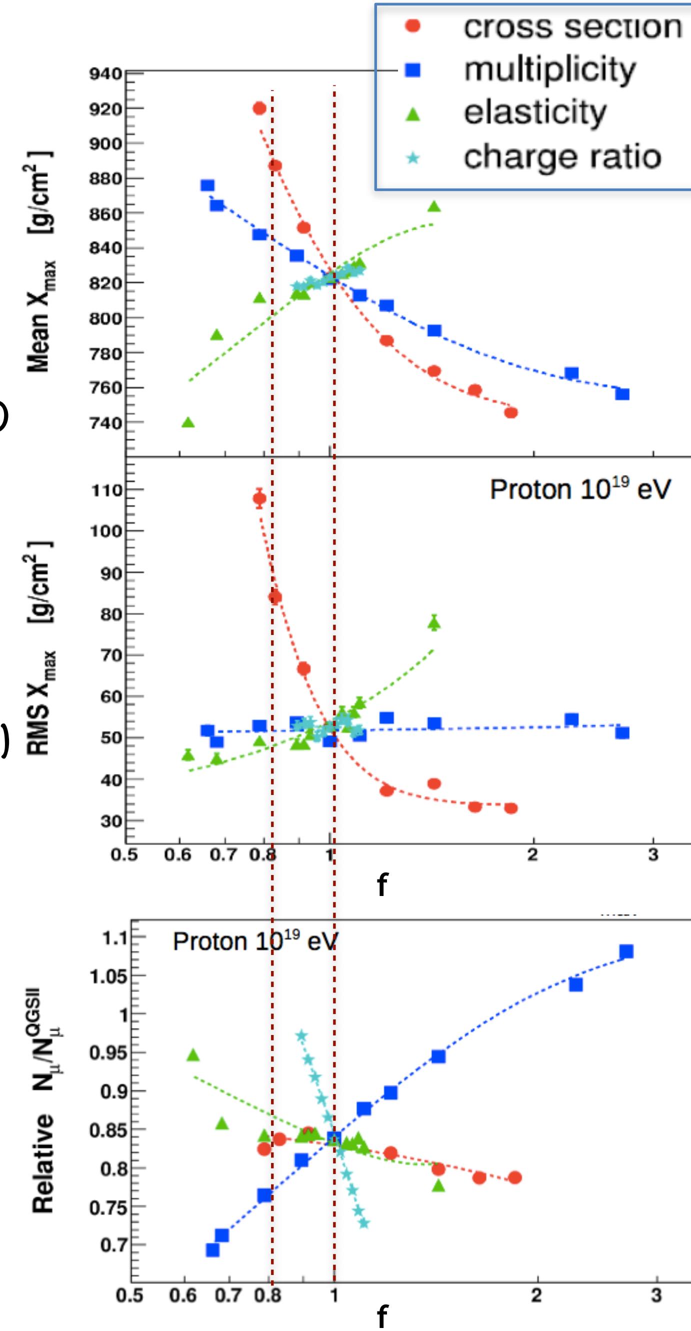

The p-Air cross section

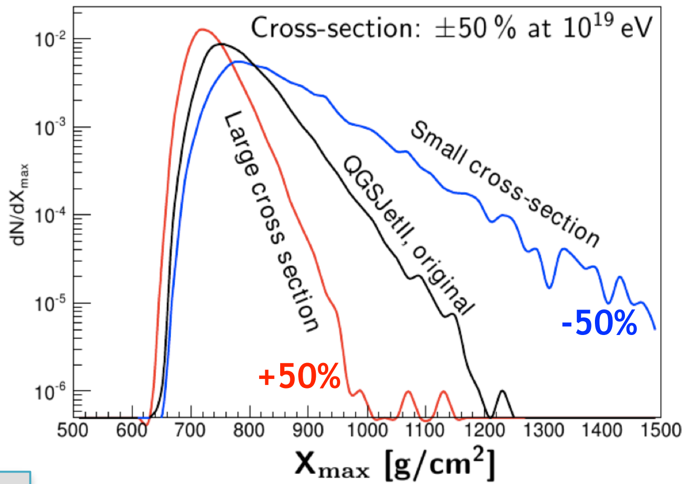

- Distribution of the depths of first interaction

$$\frac{dp}{dX_1} = \frac{1}{\boxed{\lambda_{p-Air}}} e^{-X_1/\lambda_{p-Air}}$$

- the tail of the longitudinal distribution is sensitive to the $\sigma^{inel}_{p\text{-}Air}$

$$\frac{dN_{EAS}}{dX_{max}} \propto e^{-X_{max}/\Lambda_X}$$

$$\boxed{\Lambda_X \propto \lambda_{int}}$$

[R.Ulrich, ICRC2015, arXiv:1509.03732v1]

Sys.uncertainties on $\sigma^{inel}_{p\text{-}Air}$:
+19/-25 mb in both energy ranges

- He fraction (max 25%) <18 mb
- photon fraction <5mb
- Λ_η <15 mb

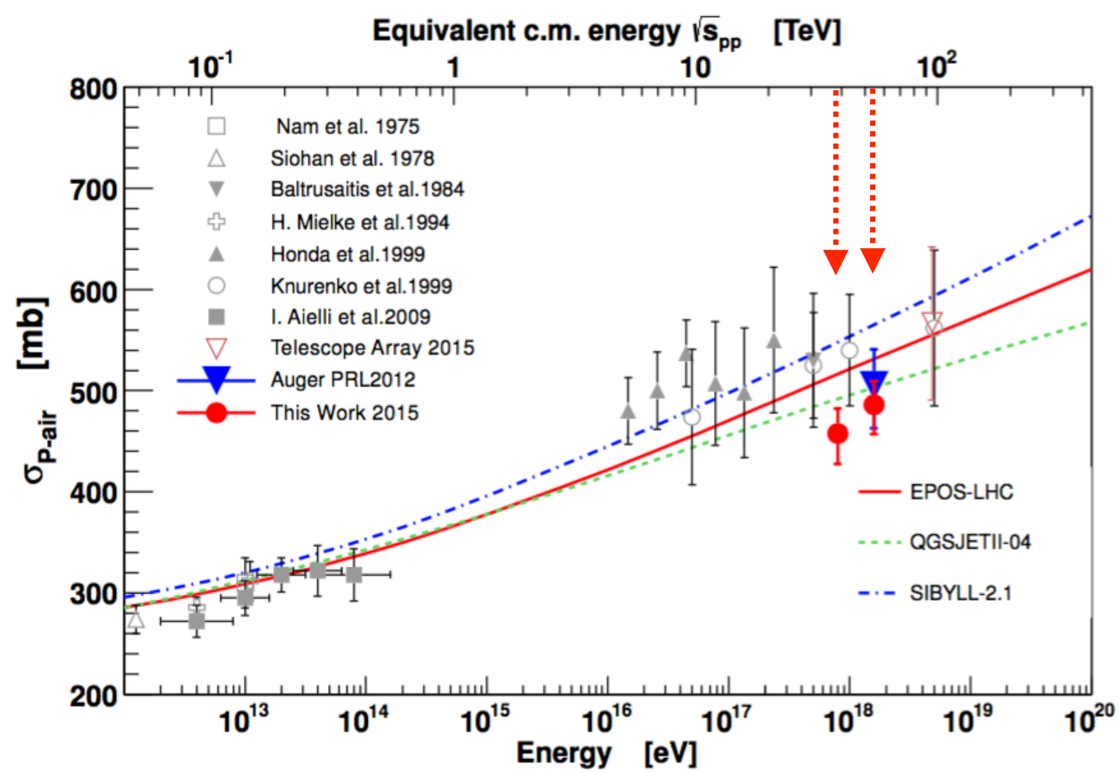

Muons to test hadronic interaction models

Muons in inclined showers

- ✓ EM component absorbed
- ✓ shape of N_μ/area almost independent of E,A,model

$$\rho_\mu^{\rm data} = \mathrm{N}_{19} \cdot \rho_\mu(\mathrm{p/QGSJ03, 10EeV})$$

PRD91 (2015) 032003; PRD91 (2015) 059991

$$\mathbf{R}_\mu = \frac{\mathbf{N}_\mu^{\mathbf{data}}}{\mathbf{N}_{\mu,19}^{\mathbf{MC}}}$$

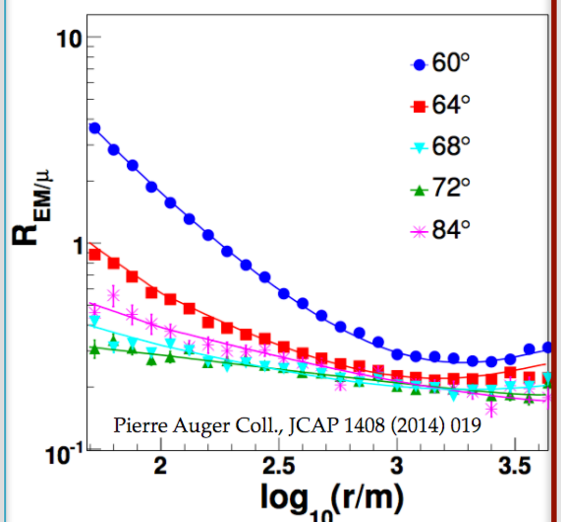

Muon content in hybrid evts

- ✓ MC evts selected to match the measured X_{max} long.profile
- ✓ ground signal components rescaled to fit data (lat.profile)
- ✓ R_E, R_{had} = energy and hadronic contribution rescale factors

[L.Collica, ICRC2015, arXiv:1509.03732v1]

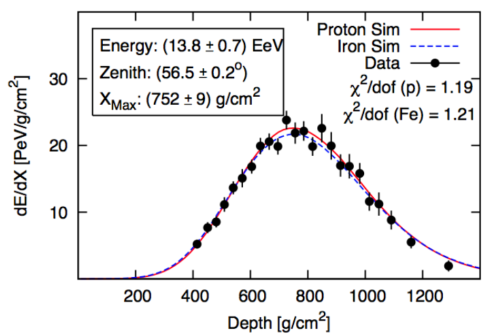

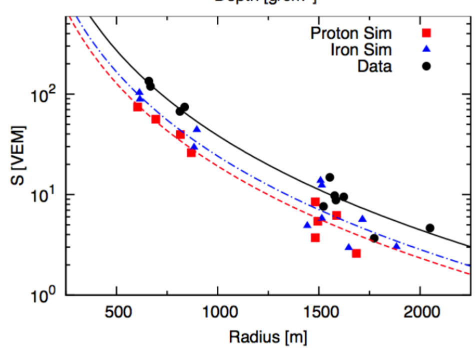

Muon production depth

- ✓ mapping of the production height by means of arrival time of muons at ground
- ✓ E>20 EeV, ϑ>55°,r>1700 m

PRD90 (2014) 012012; PRD92 (2015) 019903

$$z \simeq \frac{1}{2}\left(\frac{r^2}{c(t-\langle t_\epsilon\rangle)} - c(t-\langle t_\epsilon\rangle)\right) + \Delta - \langle z_\pi\rangle$$

$$X^\mu = \int_z^\infty \rho(z')dz'$$

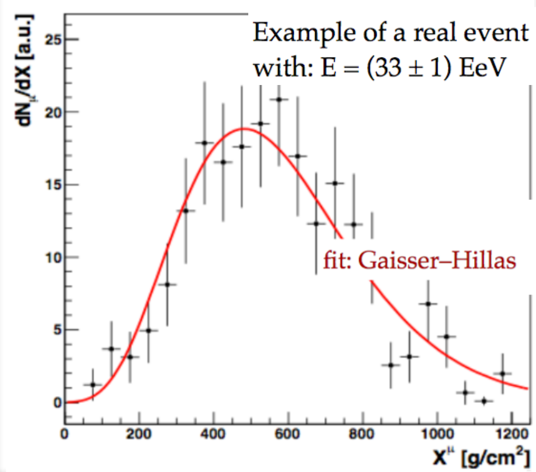

Muon content in inclined events

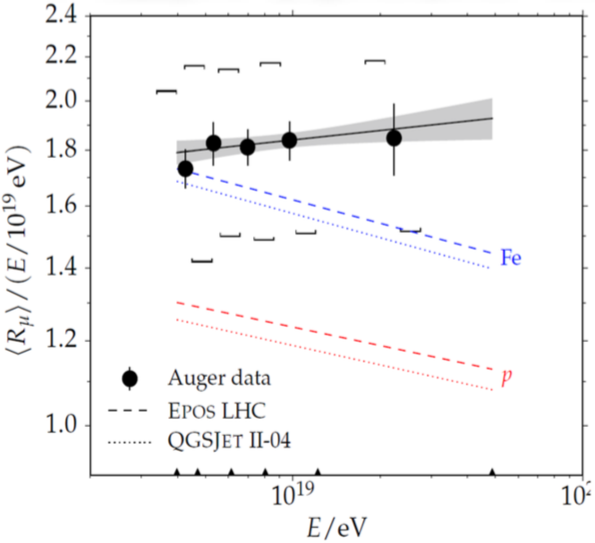

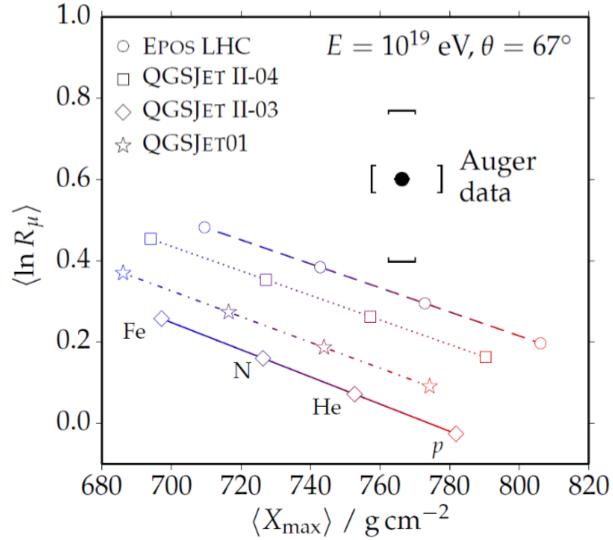

- $<R_\mu>$ higher than MC-Fe expectations
- clear tension between muon and X_{max} measurements
- largest discrepancy with pre-LHC models

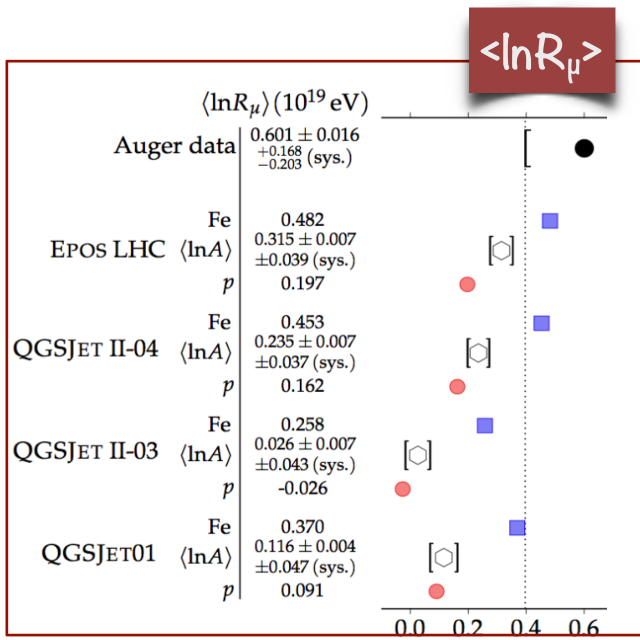

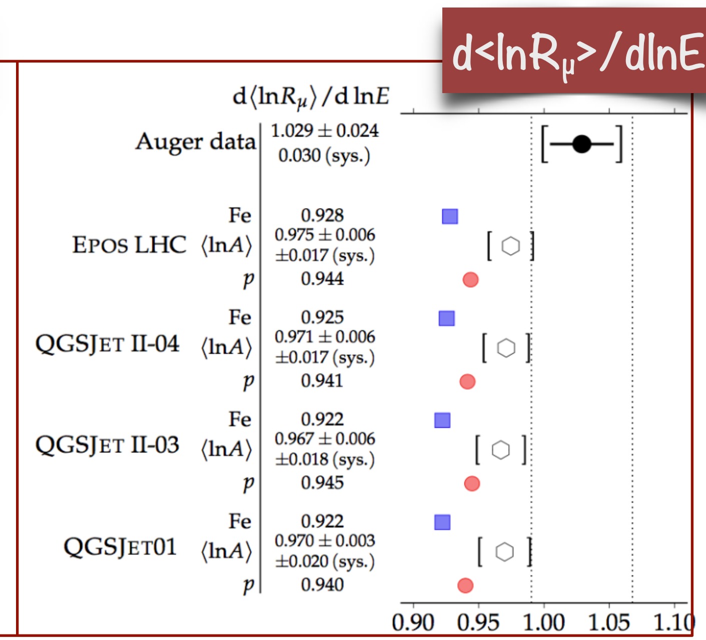

- muon deficit from 30 to 80% at 10 EeV (best for EPOS-LHC)
- deviation from constant p(Fe) at 2.2 σ (2.6 σ) level

Muon content from hybrid events

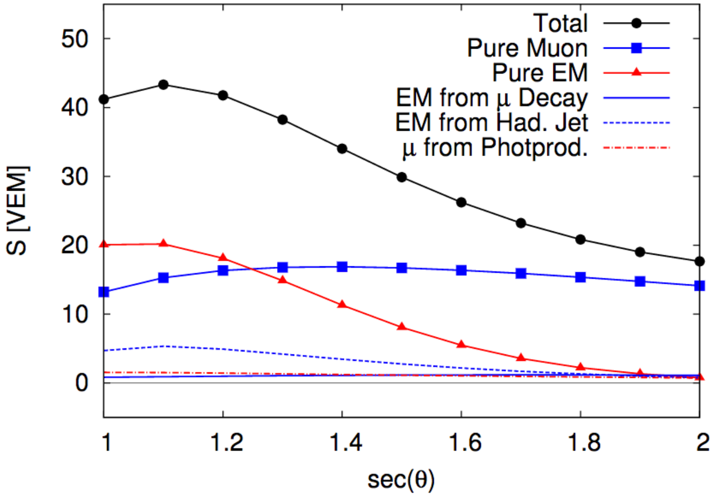

TABLE I. R_E and R_{had} with statistical and systematic uncertainties, for QGSJET-II-04 and EPOS-LHC.

Model	R_E	R_{had}
QII-04 p	$1.09 \pm 0.08 \pm 0.09$	$1.59 \pm 0.17 \pm 0.09$
QII-04 Mixed	$1.00 \pm 0.08 \pm 0.11$	$1.61 \pm 0.18 \pm 0.11$
EPOS p	$1.04 \pm 0.08 \pm 0.08$	$1.45 \pm 0.16 \pm 0.08$
EPOS Mixed	$1.00 \pm 0.07 \pm 0.08$	$1.33 \pm 0.13 \pm 0.09$

$$S_{\text{resc}}(R_E, R_{\text{had}})_{i,j} \equiv R_E\, S_{EM,i,j} + R_{\text{had}}\, R_E^{\alpha}\, S_{\text{had},i,j}$$

- no need for an energy rescaling
- observed muon signal 1.3-1.6 times larger than expected

- smallest discrepancy with prediction of EPOS-LHC for mixed composition (1.9σ level)

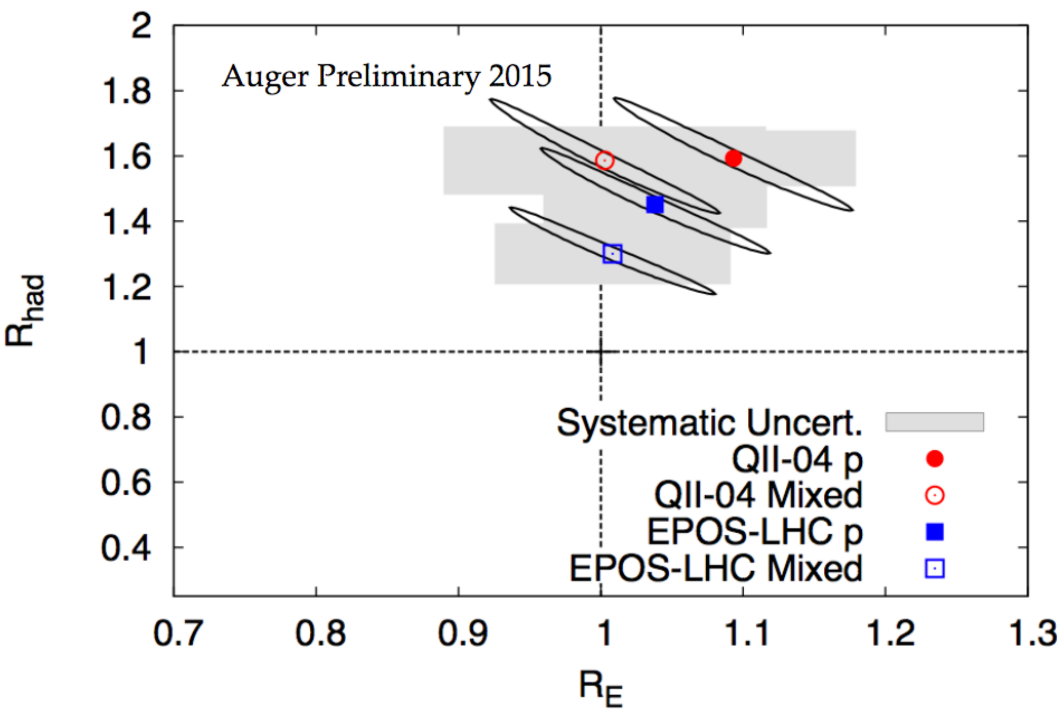

Muon Production Depth

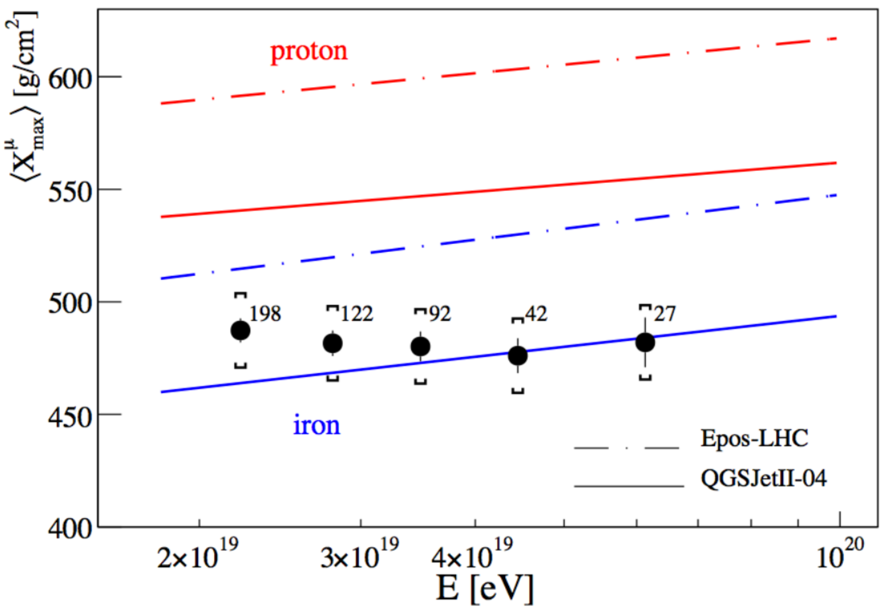

- Data bracketed by models only for QGSJetII-04
- Composition is not constant, ER~-25 g cm^{-2}/ decade
- QGSJETII-04 compatible with data within 1.5σ, EPOS-LHC incompatible at 6σ level

lnA (FD) from *Phys. Rev.* D 90 (2014) 12

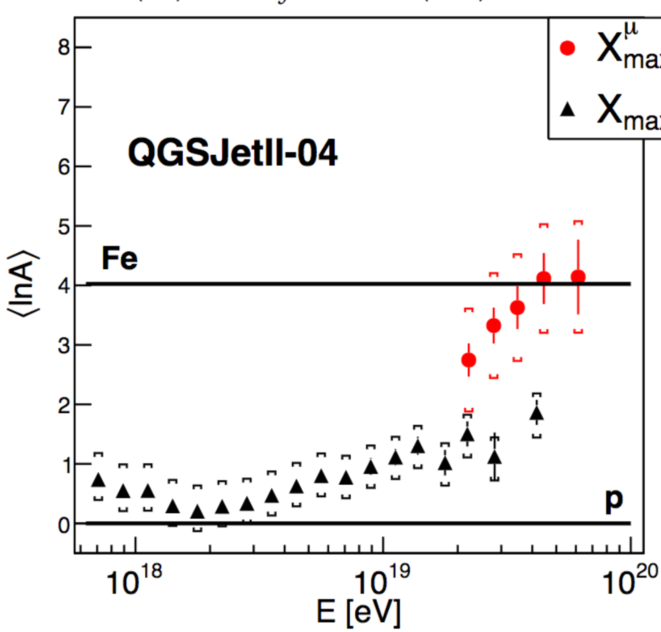

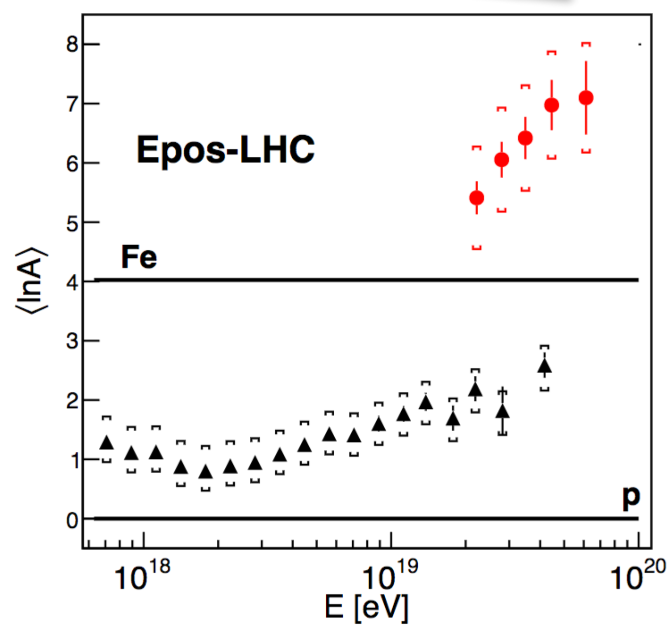

- The best model for the muon content EPOS-LHC) fails in describing the MPD

[a small change in π-Air inelasticity can induce a cumulative effect in MPD and N_{μ}^{tot}]

- **What is the origin of flux suppression ?**
  GZK, maximum injection energy at sources, others...

- **is particle astronomy feasible?**
  look for 10% protons at $E>6\ 10^{19}$ eV

- **is there new particle physics beyond the reach of LHC?**
  hadronic multi particle production, constraints...

Composition sensitivity at and above the suppression region is needed ($E>4\ 10^{19}$ eV)

⇩

AugerPrime

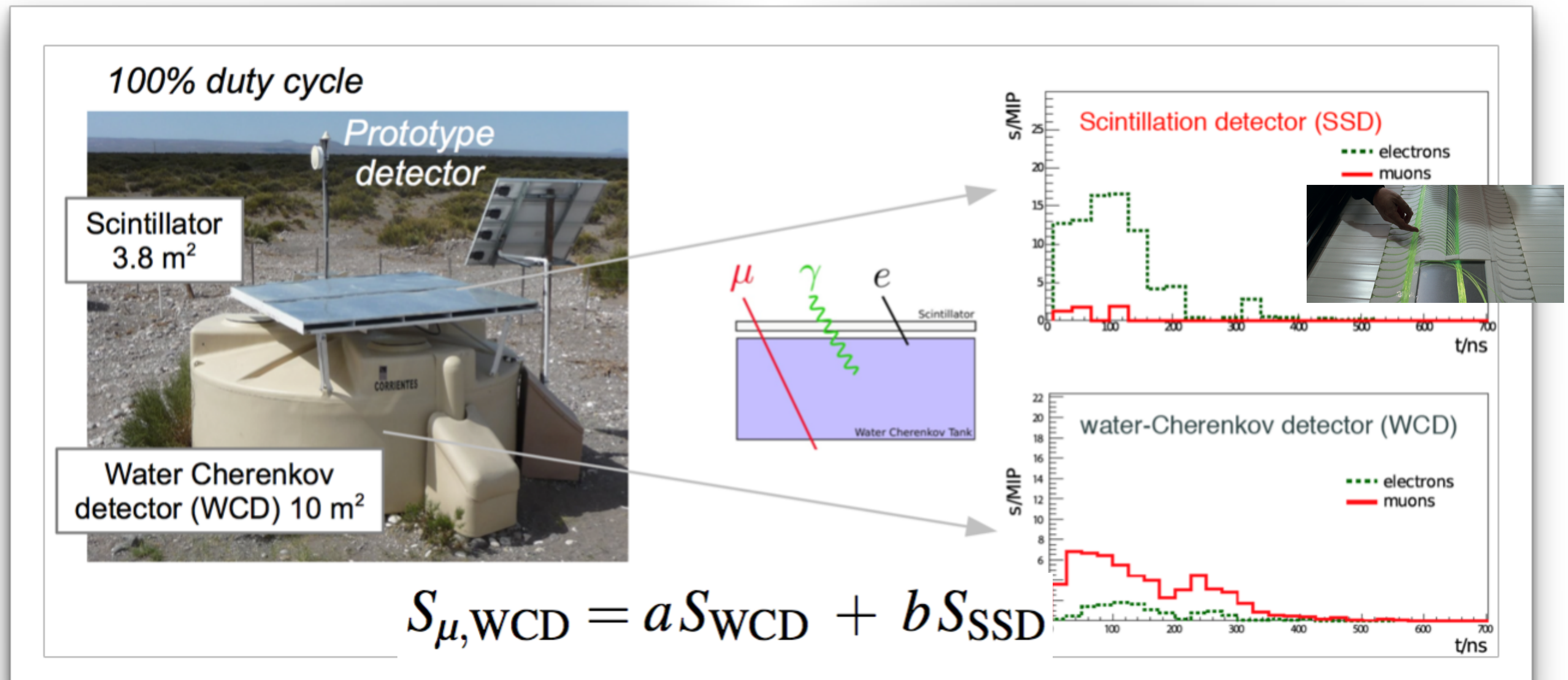

[Pierre Auger Coll., arXiv:1604.03637]

[R.Engel, ICRC2015, arXiv:1509.03732v1]

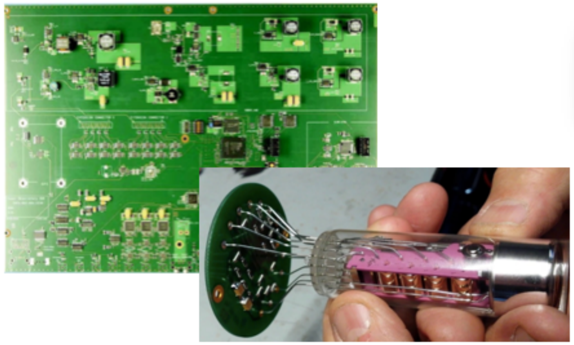

Electronics upgrade + SPMT

- faster sampling of FADC (from 40 to 120 MHz)
- more precise absolute timing accuracy (new GPS receiver)
- increase of dynamic range (+1 small PMT of 1" ⌀)

Clear sky, no moonlight *40 times higher NSB (90% moon)*

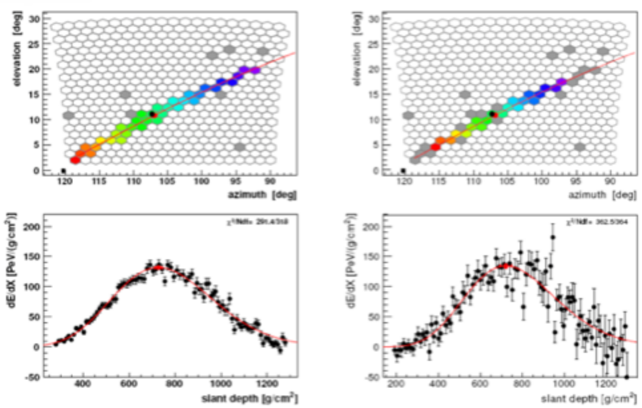

Enhanced FD operations

- measurements extended to periods of higher night sky background
- the 15% current duty cycle is increased of 50%

Underground muon detectors

- in Infill area (23.5 km2)
- direct measure of the muons
- verification of SSD

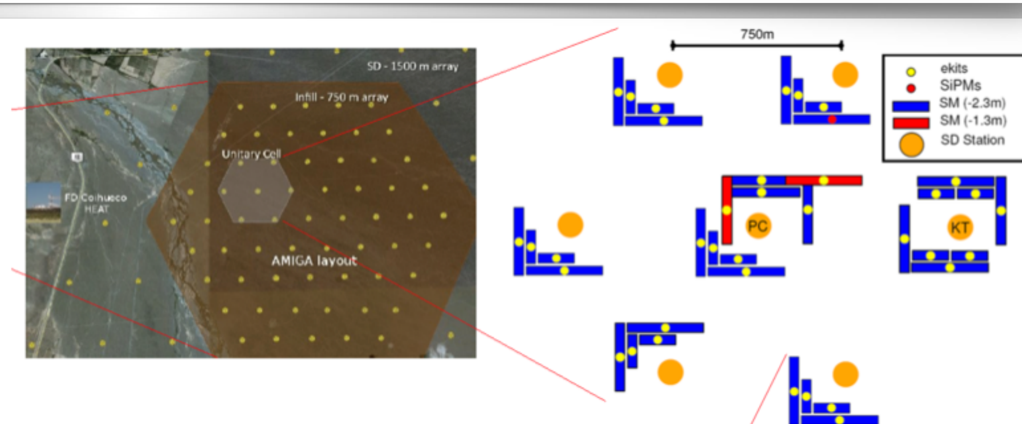

The physics goals

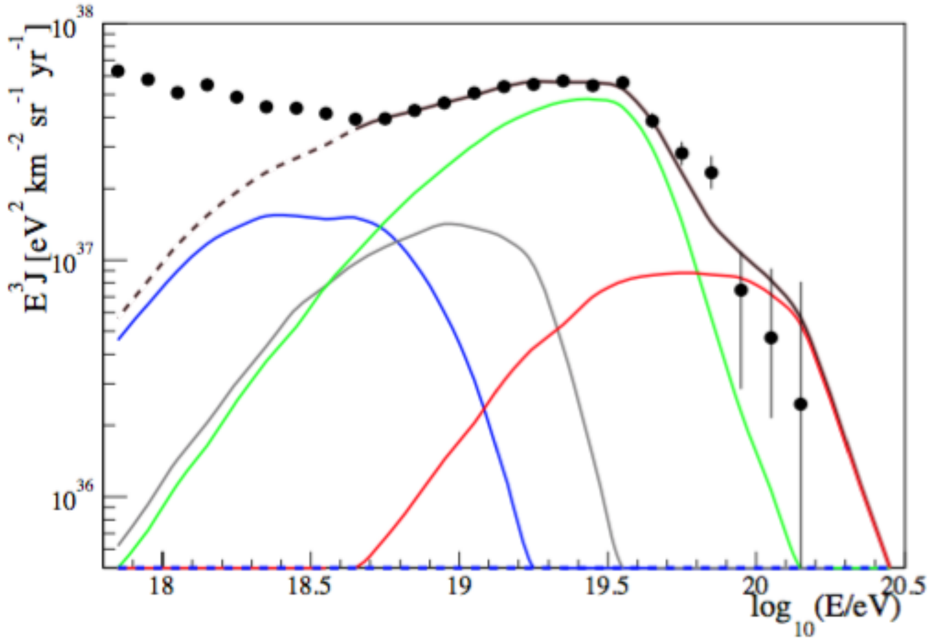

(1) - maximum rigidity model scenario

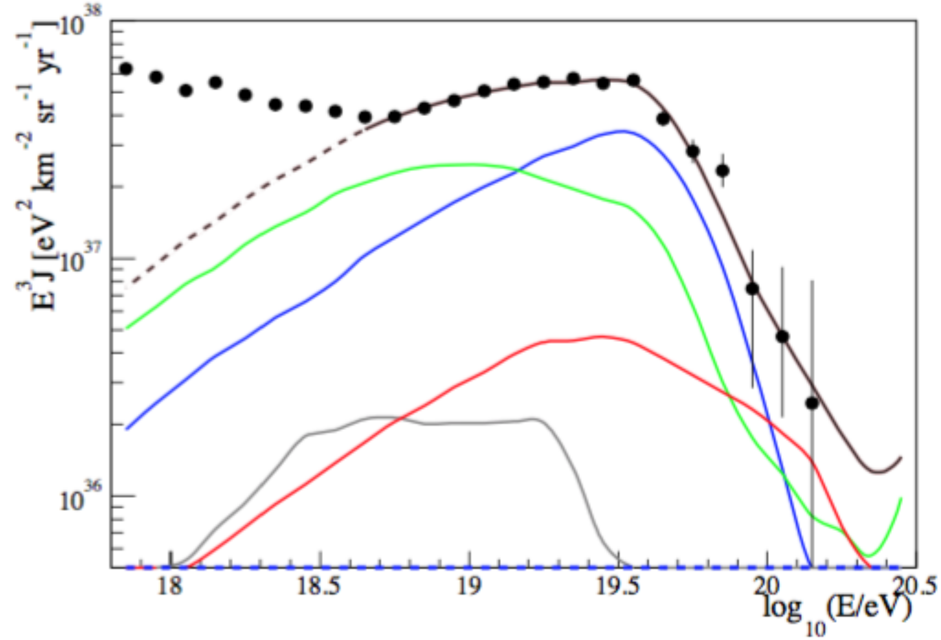

(2) photo-disintegration scenario

Mock data sets corresponding to 7 years of AugerPrime

The physics goals

Origin of the suppression

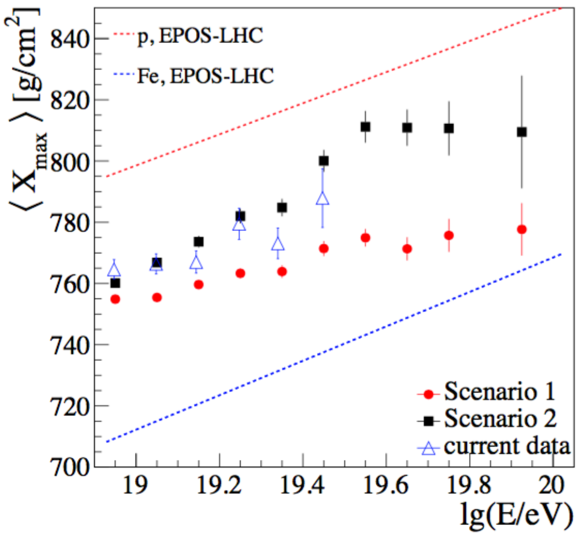

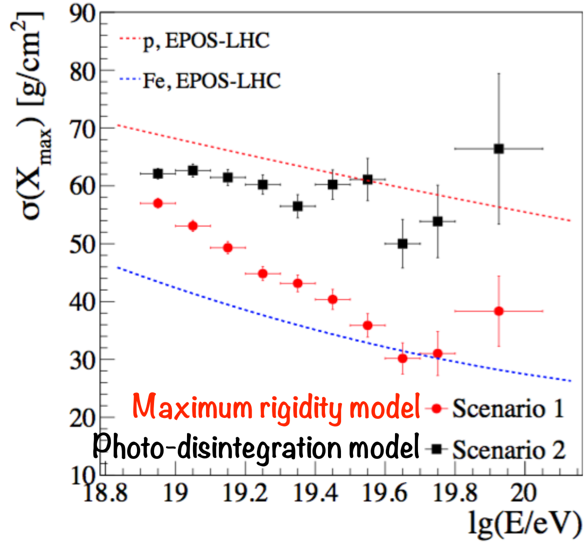

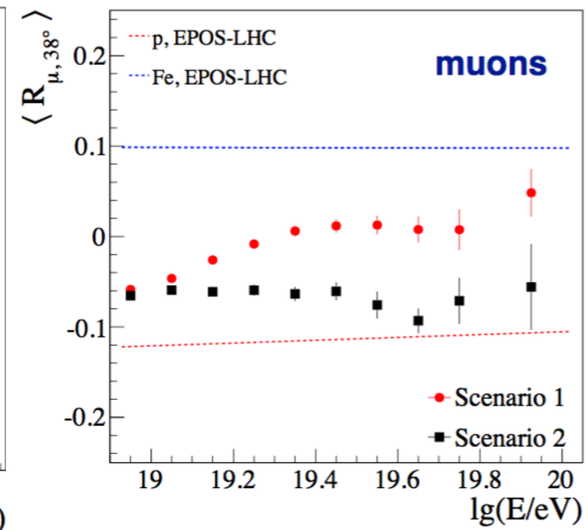

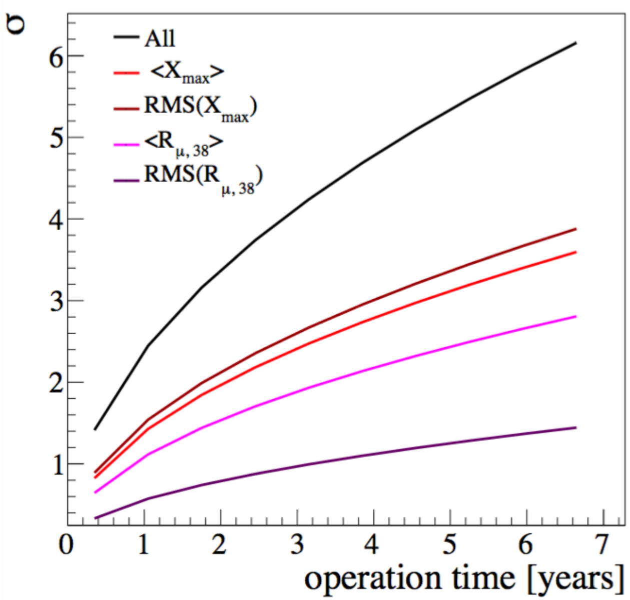

Sensitivity to proton fraction

significance of tagging scenarios with and without 10% protons (ref. scenario 1, no uncertainties due to hadronic interaction models included)

Particle physics

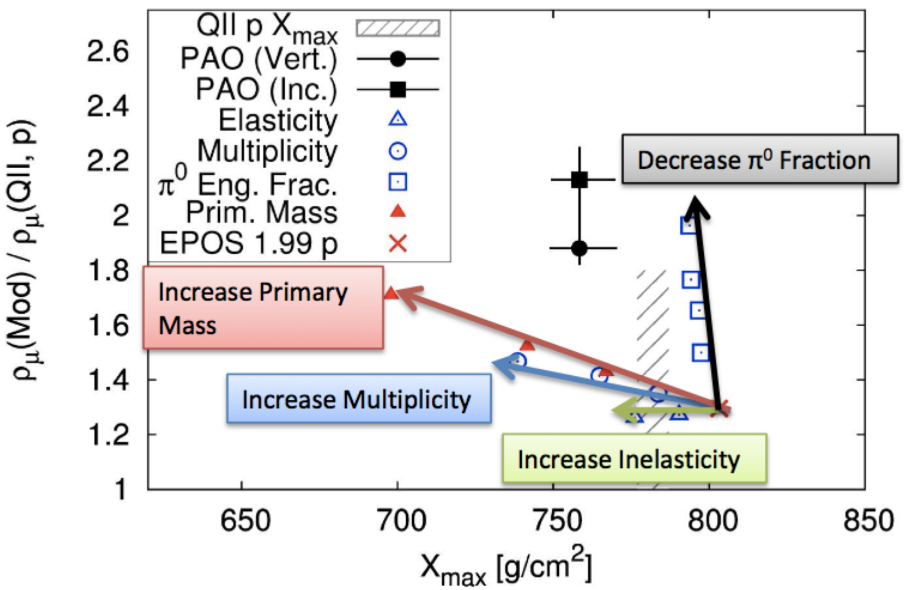

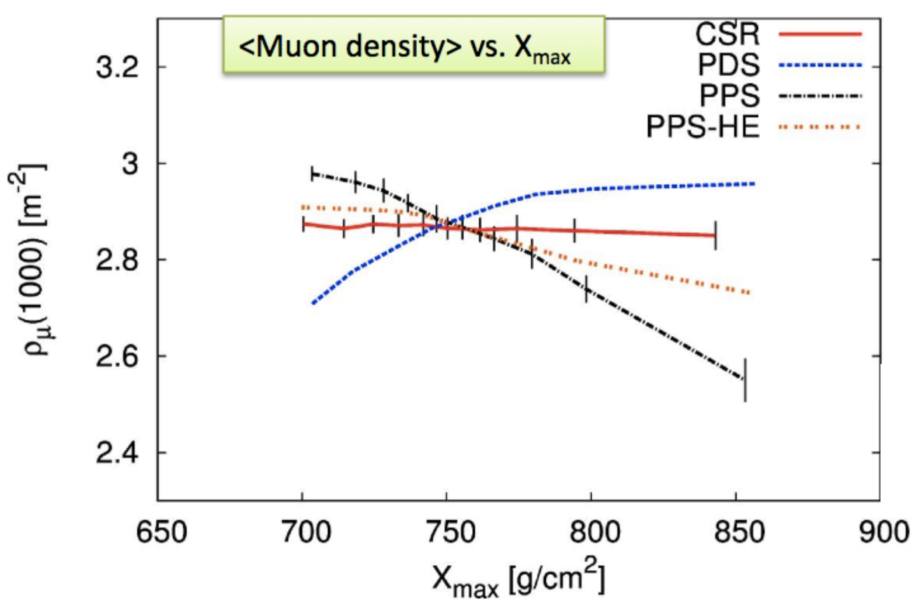

$N\mu$ → multiplicity, π^0 energy fraction, primary mass

Xmax → cross section, elasticity, multiplicity, primary mass

4 models:

CSR Chiral symmetry restoration

PDS Pion decay suppression

PPS Pion productin suppression

PPS-HE ... at high energies

From Auger...

- ✓ all particle flux suppression above 4×10^{19} EeV
- ✓ the sources of UHECRs are astrophysical
- ✓ trend towards heavier composition above $10^{18.5}$ eV
- ✓ high level of isotropy, but 7% dipole above 8×10^{18} eV
- ✓ hadr.int.models unable to reproduce measurements in a consistent way

...to AugerPrime

- ✓ extension of the composition measurements into the extreme energy range above 5×10^{19} eV
- ✓ increase of data quality (timing, dynamic range...)

Summer 2016: engineering array
Fall 2016-17 : deployment
2018-24 : data taking

Timeline

Backup slides

Correlation X_{max}-S_{1000}

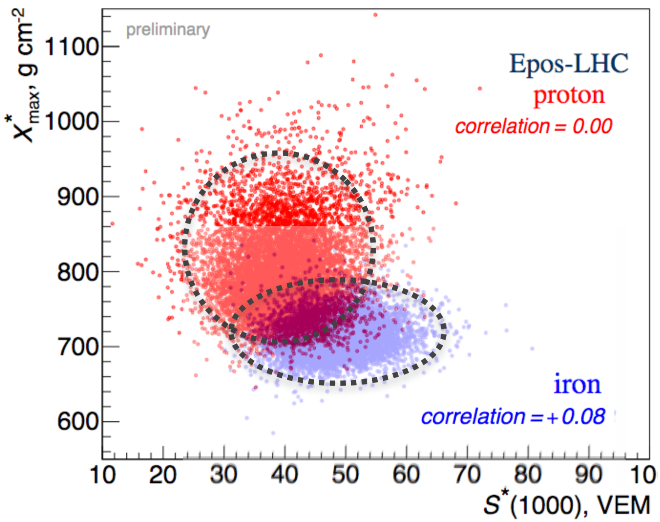

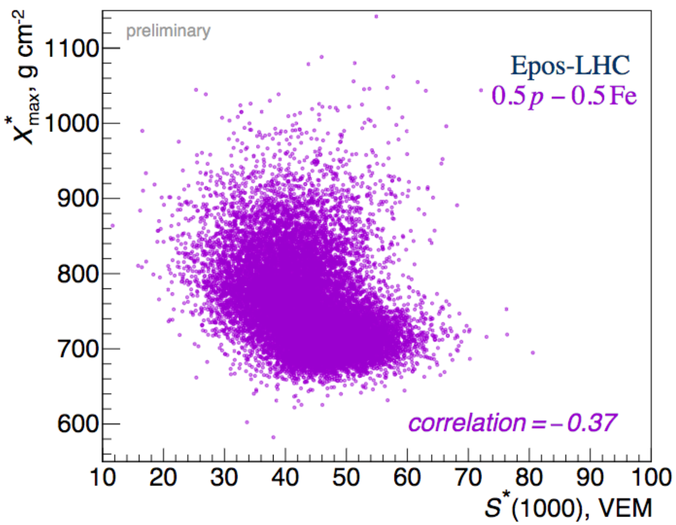

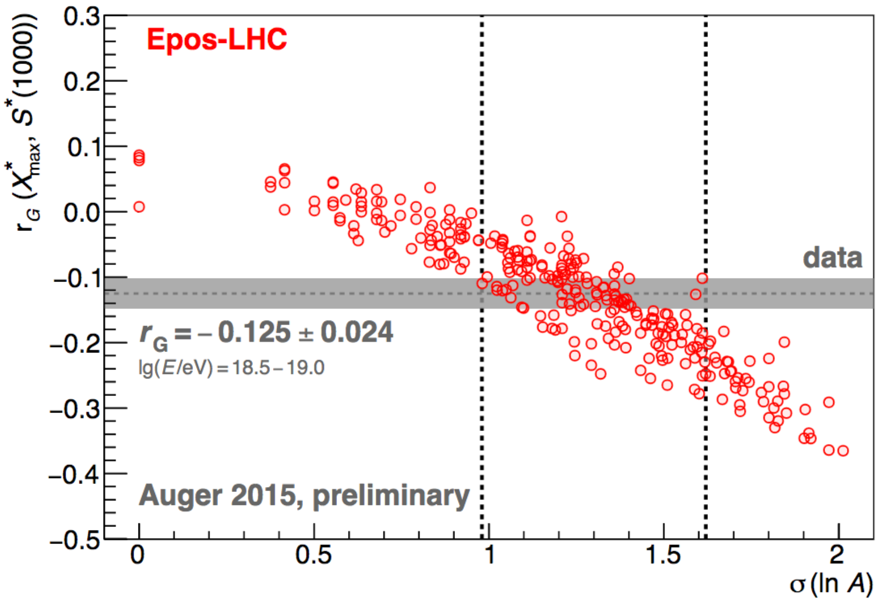

$r_{\mathrm{G}}(X^*_{\mathrm{max}},\ S^*(1000))$ for protons

Epos-LHC	QGSJetII-04	Sibyll 2.1
0.00	**+0.08**	**+0.07**

difference to data

$\approx 5\sigma$	$\approx 8\sigma$	$\approx 7.5\sigma$

difference is larger for other pure beams

- the primary composition around ankle is mixed
- difference to pure beams $\gtrsim 5\sigma$
- $\sigma(\ln A)$ compatible with data

[A.Aab et al., PRD91 (2015) 092008]

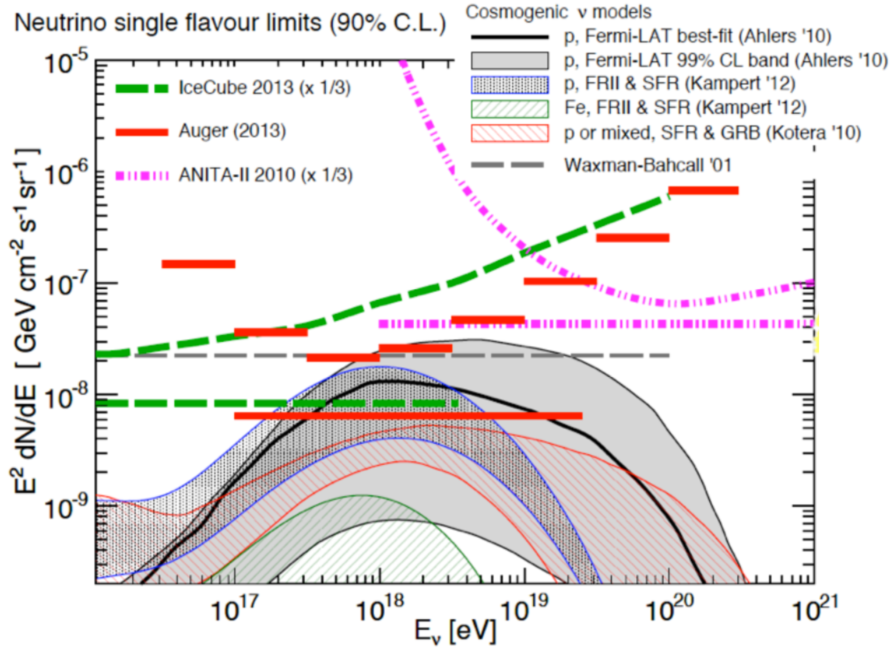

Neutrinos

$dN/dE = k\, E^{-2}$

→ **$k \sim 6.4 \times 10^{-9}$ GeV cm^{-2} s^{-1} sr^{-1}**

[0.1-25 EeV] : 90% C.L. limit
constrains models with proton primaries and strong evolution with z

[C.Bleve, ICRC2015, arXiv:1509.03732v1]

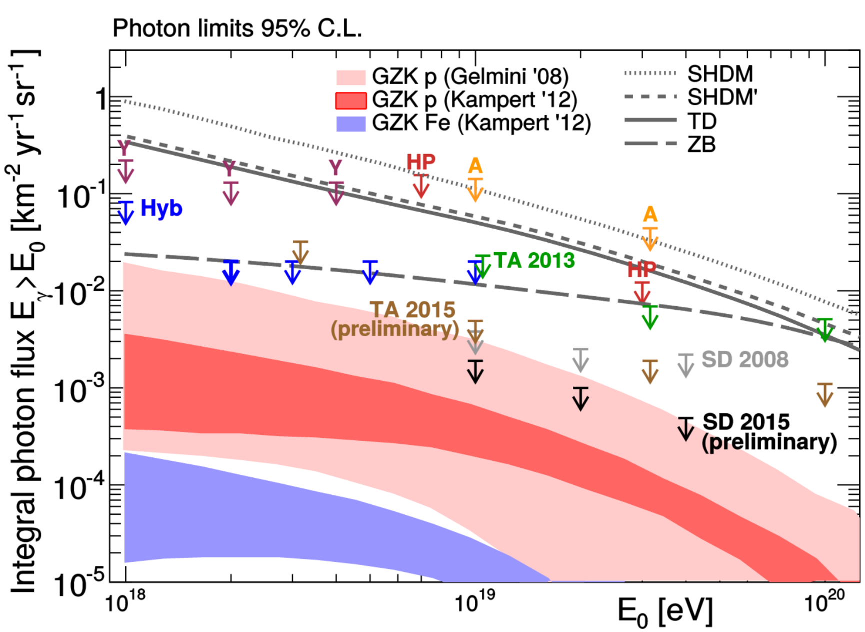

Photons

$$F_\gamma^{95\%}(E_\gamma > 10,\ 20,\ 40\ \mathrm{EeV}) < 1.9,\ 1.0,\ 0.49 \times 10^{-3}\ \mathrm{km}^{-2}\ \mathrm{yr}^{-1}\ \mathrm{sr}^{-1}$$

- 90% C.L. limit (> 10 EeV) starts to constrain models with p primaries injected at the source
- top-down models strongly disfavoured

Small & intermediate scale anisotropy tests

- astrophysical sources (photon limits on TopDown origin)
- >40 EeV (magnetic deflection $\propto Z/E$)
- O(100 Mpc) (flux suppression >20σ significance)

[J.Aublin, ICRC2015, arXiv:1509.03732v1]

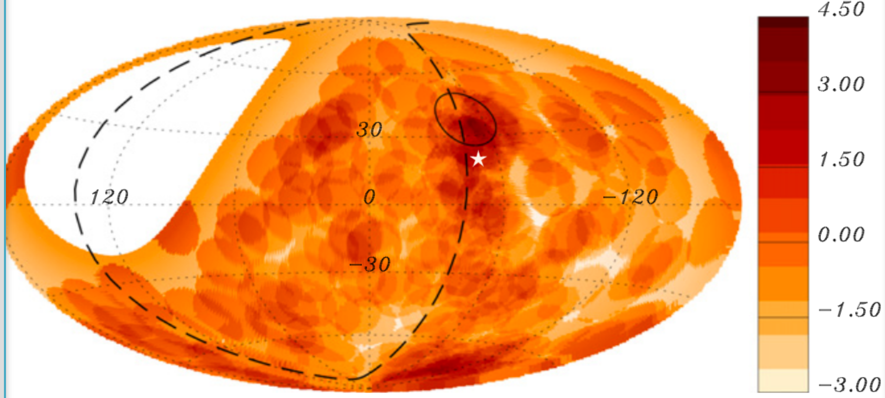

Intrinsic anisotropies

- blind searches
- autocorrelation

—> most significant excess (4.3σ): 18° from CenA

—> post-trial probability : 69%

(fraction of isotropic simulations that have a more significant excess under the same scan.)

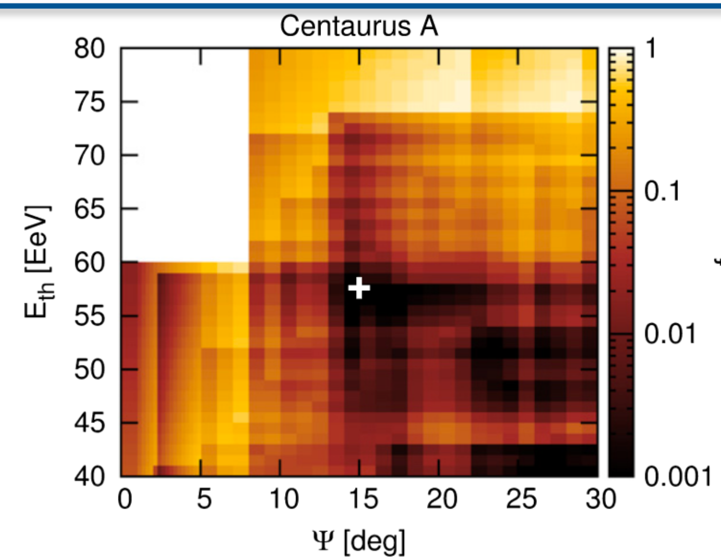

Searches with astrophysical catalogs

- 2MRS galaxies, Swift-BAT AGNs, radio galaxies, CenA
- cross-correlation counting pairs of CRs-source within angular radius Ψ

—> all tests compatible with expectations from isotropy

Large scale anisotropy tests

Harmonic analysis of counting rate (Rayleigh analysis + East-West method below 1 EeV)

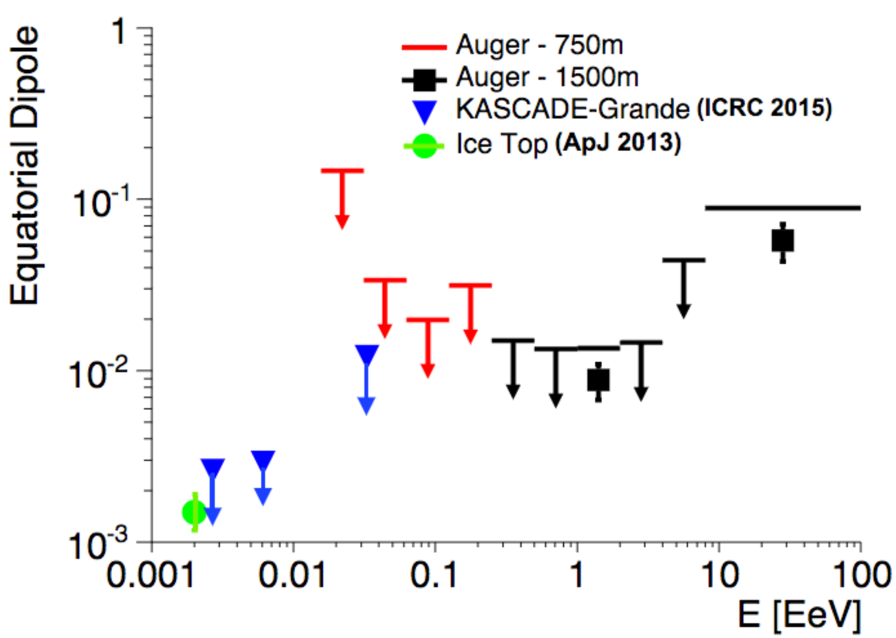

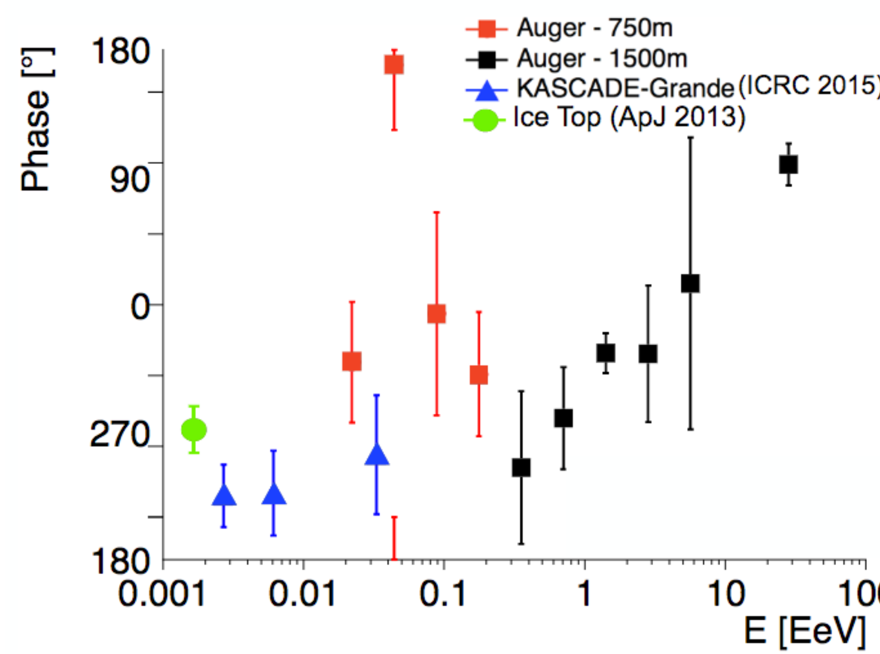

[I.al Samarai, ICRC2015, arXiv:1509.03732v1]

Amplitude upper limits ~ 1%

- exclude the presence of a large fraction of Galactic protons at EeV energies. ExtraGalactic contribution needed to explain the X_{max} results
- departure from isotropy above 8 EeV confirmed by an Auger-TA analysis (α=95°±13°, δ=-39°±13°)

Phase transition

- phase > 8 EeV opposite to the one below (pointing to the Galactic center) - random phase expected from isotropy
- extraGalactic cosmic rays progressively dominating

Event reconstruction in AugerPrime - I

Single station matrix analysis

- muon signal from $S_{\mu,\mathrm{WCD}} = a S_{\mathrm{WCD}} + b S_{\mathrm{SSD}}$
- large fluctuations, only mean muon numbers

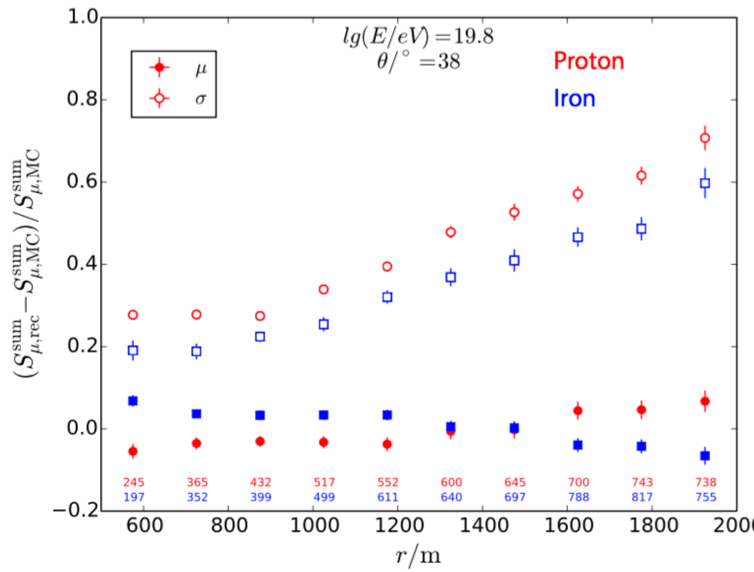

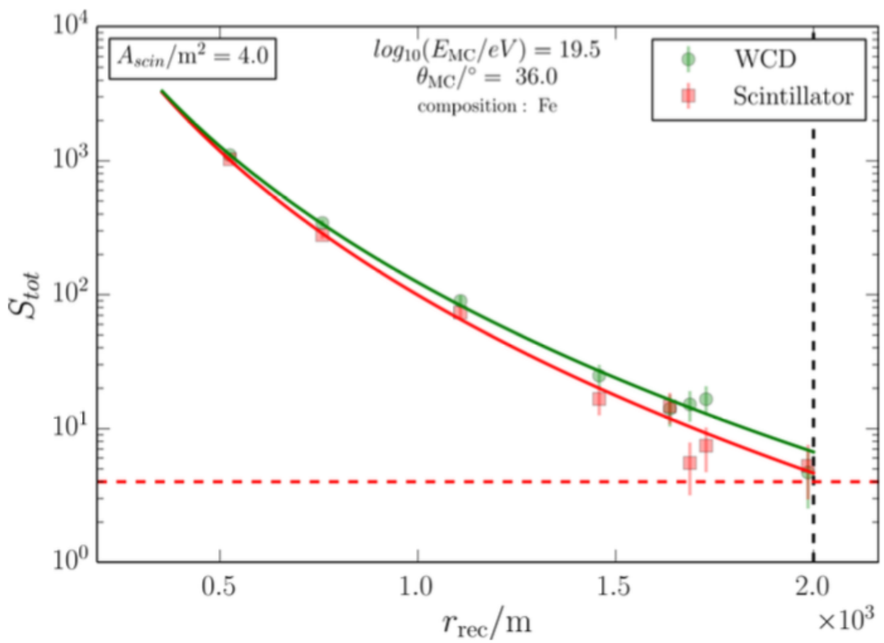

$S_\mu(800)$ from LDF

- muonic LDF derived from WCD and SSD signals
- $\dfrac{\sigma[S_\mu(800)]}{\langle S_\mu(800)\rangle} \approx 22\%(p), 14\%(Fe)$ (high E, low ϑ)

$$f_{\mathrm{p,Fe}} = \frac{|\langle S_{\mathrm{Fe}}\rangle - \langle S_{\mathrm{p}}\rangle|}{\sqrt{\sigma(S_{\mathrm{Fe}})^2 + \sigma(S_{\mathrm{p}})^2}} \sim 1.5$$

Event reconstruction in AugerPrime - II

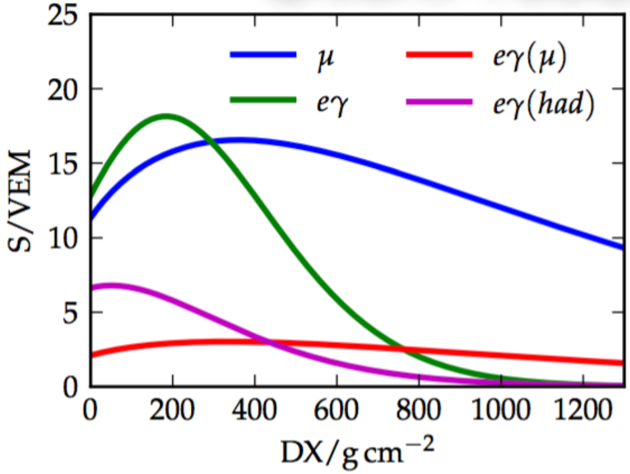

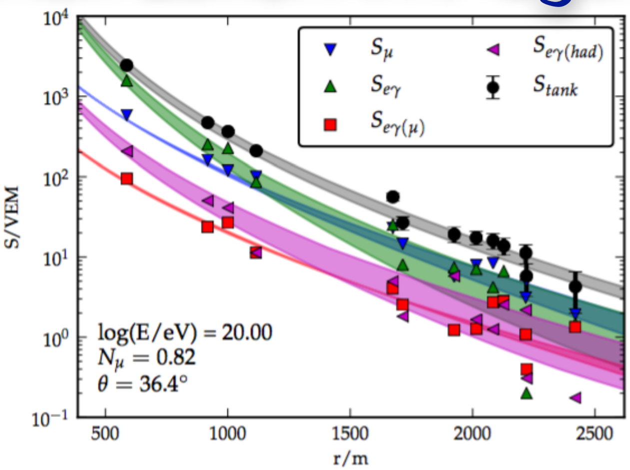

$$S_{\mathrm{tot}}(r, \Psi, DX, E, N_\mu) = S_{\mathrm{em}} + N_\mu^{\mathrm{rel}} \left[S_\mu^{ref} + S_{\mathrm{em}}^\mu \right] + (N_\mu^{\mathrm{rel}})^\alpha S_{\mathrm{em}}^{\text{collimated beam}}$$

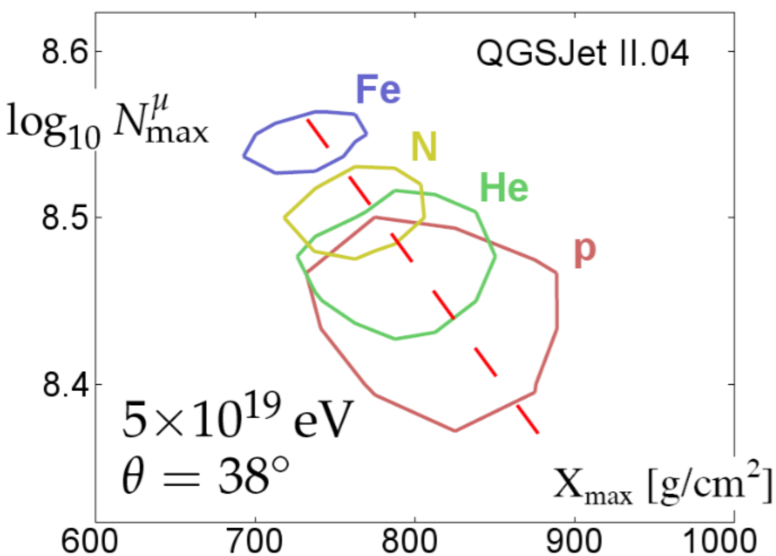

$$\frac{\sigma(X_{max})}{X_{max}} \approx 40\%(10^{19}eV), 25\%(10^{20}eV)$$

$$\frac{\sigma(E)}{E} \approx 10\%(10^{19}eV), 7\%(10^{20}eV)$$

Model	Energy	Composition	Zenith angle	$f_{\mathrm{MF}}^{\mathrm{F}}$	$f_{\mathrm{MF}}^{\mathrm{Rec}}$
QGSJetII-04	63 EeV	Proton-Iron	21°	2.08	1.56
QGSJetII-04	63 EeV	Proton-Iron	38°	1.97	1.67
QGSJetII-04	63 EeV	Proton-Iron	56°	2.14	2.1